Tesis defendida por

Armando Arce Casas

y aprobada por el siguiente comité

Dr. David Hilario Covarrubias Rosales

Codirector del Comité

Dr. Marco Antonio Panduro Mendoza

Codirector del Comité

Dr. Salvador Villarreal Reyes

Miembro del Comité

Dr. José Guadalupe Arceo Olague

Miembro del Comité

Dr. Carlos Alberto Brizuela Rodríguez

Miembro del Comité

Dr. César Cruz Hernández

Coordinador del programa de posgrado
en Electrónica y Telecomunicaciones

Dr. David H. Covarrubias Rosales

Director de Estudios de Posgrado

26 de Octubre de 2012

CENTRO DE INVESTIGACIÓN CIENTÍFICA Y DE EDUCACIÓN SUPERIOR DE ENSENADA

Programa de Posgrado en Ciencias

en Electrónica y Telecomunicaciones

Contributions to the Design and Application of Beam-forming Networks based on Coherently Radiating Periodic Structures

Dissertation

submitted in partial fulfillment of the requirements for the degree of

Doctor of Science

Presented by:

Armando Arce Casas

Ensenada, Baja California, México
2012

Abstract of the thesis presented by Armando Arce Casas, in partial fulfillment of the requirements for the degree of Doctor of Science in Electronics and Telecommunications with orientation in Telecommunications. Ensenada, Baja California, October 2012.

Contributions to the Design and Application of Beam-forming Networks based on Coherently Radiating Periodic Structures

Abstract approved by

Dr. David Hilario Covarrubias Rosales	Dr. Marco Antonio Panduro Mendoza
Co-director of Thesis	Co-director of Thesis

The increase of technologies that require advanced features in modern antenna systems such as the dynamic redirection and reorganization of its services combined with the ability to handle multiple independent beams, require solutions that integrate these characteristics efficiently. Such is the case of multiple-beam forming networks (M-BFN). In this context, a research area in modern antenna systems is associated with the reduction and simplification of the beam-forming network with the purpose of reducing the weight, size and cost of the entire antenna system.

Based on these problems, this work introduces the concept of coherently radiating periodic structures (CORPS) applied into beam-forming networks (BFN), in order to design multiple-beam forming networks. Thus, a CORPS feed network is approached as an alternative beam-forming network, efficient and innovative for multi-beam antenna systems.

Therefore, the motivation and challenge of this project was the design and study of different CORPS-BFN configurations. Including the analysis of this network in different antenna array geometries and the use of different evolutionary optimization approaches to achieve specific design goals. Similarly, one of the main goals was the introduction of the CORPS beam-forming networks and its particular features in cellular mobile communication systems as an original approach not presented in the literature previously.

Keywords: **Beam-forming network, coherently radiating periodic structures (CORPS), multiple-beam systems, beam steering, evolutionary optimization, antenna synthesis, linear and planar arrays.**

Resumen de la tesis de Armando Arce Casas, presentada como requisito parcial para la obtención del grado de Doctor en Ciencias en Electrónica y Telecomunicaciones con orientación en Telecomunicaciones. Ensenada, Baja California, Octubre 2012.

Contribuciones al Diseño y Aplicación de Redes Conformadoras de Haces basadas en Estructuras Periódicas de Radiación Coherente

Resumen aprobado por:

Dr. David Hilario Covarrubias Rosales	Dr. Marco Antonio Panduro Mendoza
Codirector de Tesis	Codirector de Tesis

El incremento de tecnologías que requieren características avanzadas en sistemas modernos de antena, tal y como la capacidad de redirigir y reorganizar sus servicios combinada con la capacidad para generar múltiples haces independientes, necesitan de soluciones que integren estas características eficientemente. Tal es el caso de redes de formación de haz de múltiples haces (M-BFN). En este contexto, un área de investigación en sistemas modernos de antena está asociada a la reducción y simplificación de la red de formación de haz con el propósito de reducir el peso, tamaño y costo del sistema completo de antenas.

Basados en estas problemáticas, en este trabajo se presenta el concepto de estructuras periódicas de radiación coherente (CORPS) aplicado a redes de formación de haz (BFN), para el diseño de redes de formación de haz de múltiples haces. De esta manera, una red de alimentación CORPS es empleada como una red de formación de haz alternativa, eficiente y novedosa para sistemas de antena multihaz.

Por lo cual, la motivación y reto de este proyecto fue el diseño y estudio de diferentes configuraciones de CORPS-BFN. Incluyendo el análisis de esta red en diferentes geometrías de agrupación de antenas y el uso de diferentes enfoques de optimización evolutiva para lograr metas específicas de diseño. Del mismo modo, una de las principales metas fue la introducción de las redes de formación de haz CORPS y sus características particulares en sistemas de comunicaciones móviles celulares como un enfoque original no presentado antes en la literatura.

Palabras Clave: **Red de formación de haz, estructuras periódicas de radiación coherente (CORPS), sistemas multihaz, direccionamiento de haz, optimización evolutiva, síntesis de antena, agrupaciones lineales y bidimensionales.**

To Nicole and María Elena

My two great loves...

Acknowledgments

I would like to express my eternal gratitude to my co-director of thesis Dr. David Covarrubias, for giving me the opportunity to develop my Ph.D. studies in the Wireless Communications Research Group. Thank you for your guidance and support through this vast sea of the research. Similarly, I owe special thanks to my co-director of thesis and friend Dr. Marco Panduro for his support, advice and for pointing me in the right direction.

I would also like to thanks to my committee members, Dr. José Arceo, Dr. Salvador Villarreal and specially Dr. Carlos Brizuela, for their comments and feedback for enrich this work.

I would like to extend my gratitude to my past and current colleagues in the Wireless Communications Research Group, specially to my partners Guillermo, Leonardo and Alejandro for their pleasant companionship and camaraderie during the past years. The interesting work related discussions, and not to forget the non-work related discussions, made every day a constant and enjoyable learning in different aspects of my life.

I am also grateful to the National Council of Science and Technology (CONACYT) and the Center for Scientific Research and Higher Education of Ensenada (CICESE) for the facilities provided for my postgraduate education including my Ph.D. degree with financial support.

Special thanks goes to my parents, Armando and Magdalena, and my sisters, Magda and Karen, for their love, encouragement and support. Most importantly, I would like to thank to my life partner, María Elena, for her love, constant support and believing in me, enriching my everyday life and giving me strength to go ahead. Likewise, my deepest thanks goes to my beloved daughter, Nicole, constant source of motivation and inspiration, who shared with me her light and joy when my mind was elsewhere.

Finally, I wish to thank friends and significant strangers who have probably forgotten me and unknowingly, helped me in this long journey in ways unknown to them.

Contents

List of Figures

List of Tables

List of Algorithms

xx

List of Abbreviations

2D CORPS-BFN	Two-dimensional CORPS-BFN, term used to refer to a CORPS system integrated by one-dimensional CORPS networks
AF	Array Factor
AoA	Angle of Arrival
BER	Bit Error Rate
BFN	Beam-forming Network
C-BFN	The same meaning of CORPS-BFN, but to refer to a specific one-dimensional network
CICESE	Center for Scientific Research and Higher Education of Ensenada from the acronym in Spanish (Centro de Investigación Científica y de Educación Superior de Ensenada)
CORPS	Coherently Radiating Periodic Structures
CORPS-BFN	Coherently Radiating Periodic Structures Beam-forming Network
D	Directivity
DE	Differential Evolution
FNBW	First Null Beamwidth or Beamwidth between First Nulls
GA	Genetic Algorithms
HPBW	Half-power Beamwidth
LSE	Least Square Error
M-BFN	Multiple-beam Forming Network
MIMO	Multiple-Input and Multiple-Output
MPM	Matrix Pencil Method
NP-Hard	Nondeterministic Polynomial-time Hard
PSO	Particle Swarm Optimization
PSP	Patch-Slot-Patch
R-node	Recombination Node
S-node	Split Node
SINR	Signal-to-Interference-plus-Noise Power Ratio
SIR	Signal-to-Interference Ratio
SLL	Side Lobe Level
SVD	Singular Value Descomposition
ULA	Uniform Linear Array
UPNA	Public University of Navarra from the acronym in Spanish (Universidad Pública de Navarra)

1. Introduction

1.1 Background

The basis of all wireless communication is based on the understanding of the phenomena of radiation and reception in antennas including the propagation of electromagnetic fields between them. These phenomena involved in wireless communications are based upon the laws of physics and can be explained through the use of Maxwell's unified electromagnetic theory.

Historically speaking[1], the theoretical foundation for electromagnetic radiation of antennas was developed by James Clerk Maxwell in 1873 combining previous work of Hans Christian Oersted, Michael Faraday, Andre Marie Ampere and Carl Fredrick Gauss. However, it was not until 1886 that Heinrich Hertz built the first radio antennas and in 1897 Guglielmo Marconi first patented a complete wireless telegraphy system being a pioneer of transoceanic radio communications.

Subsequently, the transmission of voice wirelessly occurred after the invention of the vacuum tube amplifier and oscillator between 1904 and 1915. In the stage between 1916 and 1920 the early antennas appeared in the business of broadcasting, these antennas were makeshift antennas evolved from designs used in point-to-point communication.

Just before World War II, centimeter wavelengths became common and the entire radio spectrum opened up to wide usage. At the beginning of Second World War, the conflict intensified the need for compact communication equipment and high-resolution radar[2]. The radar systems in this time employed array technology, however this tech-

---

[1]More information about the history of antennas can be found in (Balanis, 1992; Gordon, 1985; James, 1989; Kraus, 1985; Ramsay, 1981).

[2]This term is the acronym for radio detecting and ranging, system proposed by Robert Alexander Wattson-Watt in 1935.

nology to increase directivity preceded from the First World War.

In the same way, phased array antennas[3] were used in World War II. These early phased array technology use electromechanical means for the phase/time delay. In this matter, the next step (in the 1950s) was to replace the mechanically operated phase shifters by electronic phase shifters. This advance in phased array antenna technology increased switching and steering speed and thereby flexibility.

At the beginning of 1960s, reusable beam forming networks were proposed, these were multi-beam systems that maintain the isolation between its various inputs. Additionally in the same decade, digitally switched phase shifters were introduced increasing the flexibility and making it possible to electronically steer the antenna beam.

While Second World War launched a new era in antennas promoting its research, advances made in computer architecture and technology during the 1960s through the 1990s have had a major impact on the advance of modern antenna technology. Since this time, the development of novel design strategies in antennas and its feed networks to satisfy the needs of today wireless communications is an open and wide area of scientific research.

1.2   Overview of Multiple-beam Forming Systems

In order to produce multiple beams at different directions, it is necessary to feed an antenna array with multiple signal generators (or multiple receivers) simultaneously through a feed system[4]. In the feed network each input port exciting the antenna array produce one of many different beams. The purpose of the network is to transmit power to the radiators (transmit mode) or to collect signals from the antenna elements (receive

---

[3]Also known as steered beam array antennas.

[4]A feed system is a network connecting the antenna input to its radiators.

mode). This array fed or beamformer is usually called beam-forming network (BFN) or beam-forming matrix (Litva & Lo, 1996).

As mentioned earlier, design methodologies for multiple-beam forming networks were developed at the beginning of 1960s. The most significant research in the area at this time is related to the Butler matrix (Butler & Lowe, 1961), Blass matrix (Blass, 1960) and Rotman lenses (Rotman & Turner, 1963). These feed systems are briefly described below:

The Butler matrix is the most commonly used and known beam-forming network due to its performance and possible applications[5]. A Butler matrix (Figure 1) is capable of producing M beams, where M is any integral power of 2. The beam-forming matrix uses passive hybrid power dividers and fixed phase shifters to produce the desired progressive phase shifts at the elements of an antenna array necessary to form simultaneous multiple beams (one orthogonal beam per antenna element) (Butler & Lowe, 1961).

A Blass matrix is a multi-beam feed network that has M beams created from N antenna elements (Blass, 1960). This feed system (shown in Figure 2) uses a set of array element transmission lines which intersect a set of beam ports lines, with a directional coupler at each intersection. The directional couplers are equally spaced along the transmission line in such a way as to create a constant phase shift between elements in order to steer the beam to a desired location. The transmission lines are terminated in matched loads to prevent reflections but with the inconvenience of reducing efficiency.

A Rotman lens (Rotman & Turner, 1963) is a type of bootlace lens formed by two-dimensional lens with a flat front face with three focal points. Signals received from radiating feed are picked up by radiators at the back face of the lens and distributed

---

[5]This information can be found in (Chang *et al.*, 2010; Corona & Lancaster, 2003; Grau *et al.*, 2006; Jeong & Kim, 2010; Kaifas & Sahalos, 2006; Nedil *et al.*, 2006; Rose *et al.*, 2007).
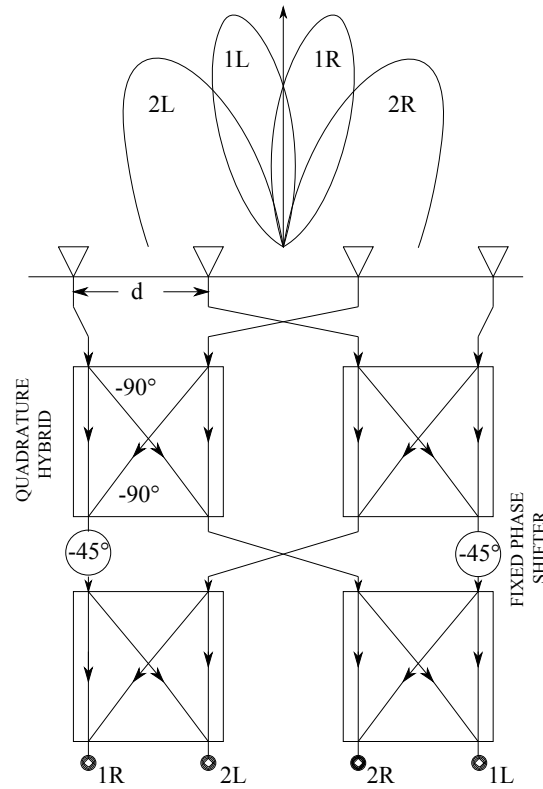
Figure 1. Butler beam-forming matrix for a four-element antenna array and radiated beams.
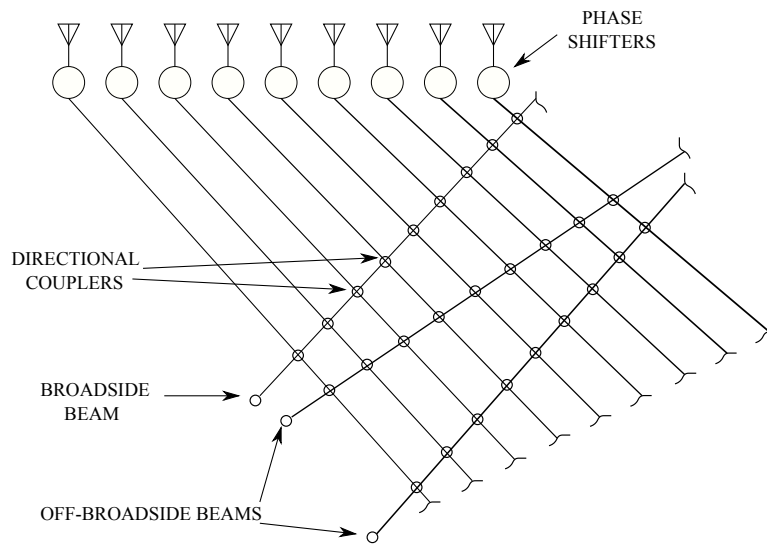
Figure 2. Constrained Blass time-delayed multiple-beam forming matrix feeding a phase-scanned array.

by transmission lines to radiate at the lens front face. Design of these kind of lenses must involve both geometric trades and mutual coupling effects between the lens ports. The latter is relatively difficult to control, but the former is essential to the realization of an efficient and compact lens. A typical diagram of a Rotman lens is illustrated in Figure 3:
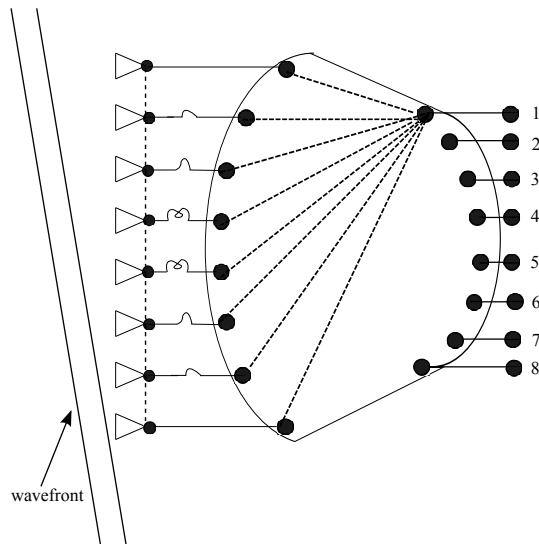
Figure 3. Diagram of a Rotman lens, ray traces and radiated wavefront.

Since the decade of 60s research on multiple-beam systems is related to hybrid technologies, specific applications and performance improvements[6]. However, the increase of technologies that require modern antenna systems has revived the interest in multiple-beam systems.

Recent technologies of multiple-beam systems involve smart antennas (Sarkar *et al.*, 2003) and MIMO[7] (Döttling *et al.*, 2009) systems for many different applications. This kind of technologies exploit the high versatility of multiple-beam systems, such as the dynamic redirection and reorganization of its services combined with the ability to handle multiple beams.

---

[6]References: (Fonseca, 2009; Jeong & Kim, 2010; Kaifas & Sahalos, 2006; Rose *et al.*, 2007).

[7](Multiple-Input and Multiple-Output) is an antenna technology for wireless communications.

The most recent research in multiple-beam forming networks is based on the fundamental principles of periodic structures (Betancourt & del Rio Bocio, 2007). This new feed system is known as Coherently Radiating Periodic Structures beam-forming network (CORPS-BFN) and offers improvements based on properties of this kind of structures. This new proposal is an open research area and therefore has been studied in the last couple of years as described in the next section.

1.3   State of the Art

Since the introduction of coherently radiating periodic structures (CORPS) technology efforts have been made to promote this technology in different areas of research for various applications. However, the literature concerning CORPS is still scarce and the potential of the network for its use in various applications is not yet exploited.

Early attempts of the study of periodic structures as a beam-forming network to feed antenna arrays is proposed in (Betancourt & del Rio Bocio, 2007), this work introduces a methodology to reduce the complexity of the associate control of a bidimensional phased array for scanning the main beam to any desired direction. This similar approach is studied briefly for linear arrays in (Betancourt & del Río, 2006). However, the CORPS technological concept was introduced for first time and applied to high-resolution imaging systems in (Garcia *et al.*, 2005). The earliest applications of CORPS structures involved obtaining images (Gomez & del Rio, 2006) and the use of PSP (Patch-Slot-Patch) to improve the radiation features of arrays increasing the directivities of each one of the beams keeping the original phase centers (Betancourt & del Rio, 2009).

Furthermore, in (Betancourt & del Rio Bocio, 2007) is evidenced the complexity

for generating a radiation pattern with desirable characteristics using a CORPS-BFN. This is a complex problem that can be properly addressed by evolutionary optimization techniques[8] and is comparable in some way with the conventional antenna pattern synthesis (Panduro & del Rio-Bocio, 2009).

Thus, evolutionary optimization was introduced in the design of a CORPS feed system for linear arrays (Panduro, 2007; Panduro & del Rio Bocio, 2008; Panduro & del Rio-Bocio, 2009) using Genetic Algorithms (GA) and Differential Evolution (DE). In (Panduro, 2007) the CORPS structures are used in uniform and non-uniform linear antenna arrays and the design of CORPS networks considering several layers in this same geometry is presented in (Panduro & del Rio-Bocio, 2009), in both cases the GA algorithm is used as optimizer. The optimization of the CORPS-BFN with Differential Evolution is tackled in (Panduro & del Rio Bocio, 2008), analyzing different multi-beam configurations of CORPS-BFN in one dimension.

The CORPS technology is maturing to be introduced to new applications. Therefore, this thesis adopts this technology as the cornerstone for further contributions to the state of the art as is explained in the next section.

1.4   Motivation for Beam-forming Network Design

CORPS beam-forming networks represent the state of art in multi-beam systems. These multiple-beam forming networks are an emerging technology solution for systems requiring dynamic and reconfigurable multi-beam environments. Furthermore, an open research area in modern antenna systems is associated with the reduction and simplification of the beam-forming network with the purpose of reducing the weight, size and

---

[8](Hoorfar, 2007; Jin & Rahmat-Samii, 2007; Karimkashi & Kishk, 2010; Rahmat-Samii *et al.*, 2012; Robinson & Rahmat-Samii, 2004; Rocca *et al.*, 2011; Weile & Michielssen, 1997).

cost of the entire antenna system.

In this context, one of the most notable advantage of CORPS-BFN is the combination of phased array and multiple-beam forming network technologies, i.e. the feed system is capable of handling multiple orthogonal beams with the possibility to steer each beam dynamically. In addition, the CORPS-BFN is a feed network of less complexity in terms of hardware, in comparison with traditional beam-forming networks (e.g., Butler matrix, Blass matrix, etc.). Therefore, a CORPS-BFN could obtain desirable features in various applications such as satellite systems, cellular mobile communication systems, among others.

Based on these premises, the original contributions of this project are directed in the study of the behavior of different design configurations of CORPS-BFN including the analysis of the network in different array geometries. Similarly, due to the degrees of freedom handled in the feed network the adaptation of new evolutionary approaches applied to the beam-forming network could be considered essential and as potential contribution. Thus, one of the main motivation or goal is to introduce the CORPS-BFN in cellular mobile communication systems as an original approach that has not been presented previously in the literature.

For the motivations mentioned above, the scope addressed in this thesis involves the design and optimization of CORPS-BFN configurations in different array geometries. The above with the purpose of obtaining design features desirable in various applications of antenna including cellular mobile communications.

1.5 Objective

The main objective in this thesis is the design of beam-forming networks based on Coherently Radiating Periodic Structures and stochastic optimization methods for multiple-beam antenna systems in modern applications of antenna.

1.6 Publications

The main contributions of this work are reflected in a list of papers published during the period of research of the author in the Wireless Communication Research Group of the Electronics and Telecommunications Department, at CICESE Research Center. The publications are listed below:

- Arce, A., Yepes, L. F.,Covarrubias, D. H., & Panduro, M. A. (2012). A new approach in the simplification of a multiple-beam forming network based on CORPS using compressive arrays. *International Journal of Antennas and Propagation*, *2012*, 1-8. doi:10.1155/2012/251865

- Arce, A., Covarrubias, D. H., Panduro, M. A. & Garza, L. A. (2012). A new multiple-beam forming network design approach for a planar antenna array using CORPS. *Journal of Electromagnetic Waves and Applications*, *26*(2-3), 294-306.

- Arce, A., Covarrubias, D. H., & Panduro, M. A. (2012). Design of a multiple-beam forming network using CORPS optimized for cellular systems. *International Journal of Electronics and Communications (AEÜ)*, *66*(5), 349-356. doi:10.1016/j.aeue.2011.08.011

- Arce, A., Covarrubias, D. H., Panduro, M. A. & Garza, L. A. (2012). Design of beam-forming networks for multibeam antenna arrays using coherently radiating periodic structures. *Journal of Applied Research and Technology*, *10*(1), 48-56.

- Arce-Casas, A., Covarrubias-Rosales, D. H., & Panduro-Mendoza, M. A. (2011). Design of multibeam CORPS-BFN for cellular mobile communications systems. In *Proceedings of the 5th European Conference on Antennas and Propagation (EUCAP)*, 1272-1276.

- Arce, A., Covarrubias, D. H., & Panduro, M. A. (2011). Performance evaluation of stochastic algorithms for linear antenna arrays synthesis under constrained

conditions. *Journal of Selected Areas in Telecommunications*, *2*(5), 41-47.

- Arce, A., Covarrubias, D. H., & Panduro, M. A. (2009). Performance evaluation of population based optimizers for the synthesis of linear antenna arrays. In *Proceedings of the 6th IASTED International Conference on Antennas, Radar, and Wave Propagation (ARP)*, 103-108.

1.7   Organization of this Thesis

The structure of the thesis is shown in the block diagram of Figure 4. Chapter 2 presents the theoretical foundations of antenna arrays and evolutionary optimization. The formulation of the antenna synthesis problem and two well-known metaheuristics (genetic algorithms and particle swarm optimization) as a tool in the antenna synthesis are also presented in the second chapter. In Chapter 3, beam-forming networks based on coherently radiating periodic structures are addressed, including the CORPS-BFN theoretical model and two-dimensional CORPS networks. Next, the design of multiple-beam forming networks based on CORPS for antenna arrays is presented. Specifically, approaches based on CORPS feed networks in linear and planar arrays and additional one based on compressive arrays are discussed. This main topic is divided in two chapters. In the first part (Chapter 4), the mathematical modeling for the different approaches is described. Followed by case studies of these approaches, presented in Chapter 5. Afterwards in Chapter 6, multiple-beam forming networks using CORPS and optimization algorithms are introduced in a cellular mobile communication system. Finally, Chapter 7 concludes the thesis with a summary of its main contributions and a brief overview of related future research.

Overview

State of art

Chapter 1

Motivation for BFN design

Objective

Arrays basics

Metaheuristics in the antenna synthesis

Chapter 2

Arrays and evolutionary optimization fundamentals

The synthesis problem

CORPS-BFN model

Chapter 3

CORPS beam-forming networks

2-D CORPS-BFN

Linear Arrays

Planar Arrays

Chapter 4

Part I - Mathematical modeling

Design of CORPS-BFN for multi-beam antenna arrays

Chapter 5

Part II - Case studies

C-BFN +MPM

Chapter 6

CORPS-BFN on cellular systems

Chapter 7

Final discussion, conclusions and future research

Figure 4. Structure of the thesis.

2. Fundamentals of Antenna Arrays and Evolutionary Optimization

2.1 Introduction

This chapter explains briefly the fundamentals of two interrelated topics: the antenna array subsystem and evolutionary optimization as a tool for the antenna pattern synthesis. It is not intended to cover all the concepts and variants in both related topics but those most interesting for the development of this work.

The concept of beam-forming network is closely linked to the antenna array. In fact, the beam-forming network is in charge of feeding the array, in order to radiate one or more beams with predefined characteristics. Such characteristics can be the directivity, side lobe level, null position or main beam steering (design parameters). In antenna pattern synthesis, the control of this design variables at the same time results in a complex problem and in which stochastic optimization algorithms can obtain an appropriate solution.

Thus, one of the main advantages of antenna arrays is the ability to control the feeding of the array. The controlled feeding can obtain low side lobe level or even a shaped radiation pattern according to design specifications, function that can be performed by the beam-forming network using stochastic algorithms as optimizers.

2.2 Array Fundamentals

Antenna arrays are composed of a collection of two or more equal antennas arranged in space radiating (or receiving) simultaneously to establish a unique directional radiation

pattern. Arrays offer the unique capability of electronic scanning of the main beam. By changing the amplitude and phase of the exciting currents in each element antenna of the array, the radiation pattern can be scanned and shaped through space. This type of antenna array is know as phased array[9] (Mailloux, 1994).

A radiation pattern of the array is a graphical representation of the radiation (in most cases in far-field[10]) properties of each individual antenna element as a function of space coordinates. The radiation pattern of an array can be determined at least by the following design variables that can be used to shape the overall pattern (Balanis, 1997):

- Geometry of the overall antenna array
- Amplitude excitation of the individual elements
- Phase excitation of the individual elements
- Spacing among antenna elements
- Relative pattern of the individual elements

The radiation pattern (normalized field pattern) can be written as the product:

$$F(\theta, \phi) = g(\theta, \phi)\text{AF}(\theta, \phi) \tag{1}$$

where $g(\theta, \phi)$ is the element pattern and $\text{AF}(\theta, \phi)$ is the array factor. The element pattern is the field intensity of a single radiating element in terms of the type of the antenna. The array factor is the resulting radiation pattern if it is considered that each element of the array is an isotropic point source. The analysis of an antenna array is

---

[9]A phased array is defined as an array antenna whose main beam maximum direction is controlled by varying the phase or time delay to the elements.

[10]Also know as Fraunhofer region, defined as the region of the field of an antenna where the angular field distribution is essentially independent of the distance from the antenna.

frequently characterized by its array factor because only by multiplying the result by the proper element pattern will be enough to extend the conclusions to any other type of radiating element.

2.2.1 Radiation pattern parameters

Typical power patterns are shown in Figure 5, a linear two-dimensional pattern is illustrated in (a) and a symmetrical three-dimensional polar pattern in (b). The main lobe (main beam) is the lobe containing the direction of maximum radiation. Any lobe other than the main lobe is called minor lobe (side lobe). The relation between the main lobe and the minor lobes is referred as side lobe level (SLL). Formally, the side lobe level is the ratio, expressed in decibels, between the value of the pattern in the direction of maximum radiation $|F(\text{max})|$ and in the direction of the maximum side lobe $|F(\text{SLL})|$, and is given by (Stutzman & Thiele, 1998):

$$\text{SLL}_{\text{dB}} = 20 \log \frac{|F(\text{SLL})|}{|F(\text{max})|} \tag{2}$$

For a normalized pattern, $|F(\text{max})| = 1$. The width of the main beam is quantified through the half-power beamwidth (HPBW) or beamwidth between first nulls (FNBW). The half-power beamwidth is the angular separation of the points where the main beam of the power pattern equals one-half the maximum value. In the same way, FNBW is the angular separation of the space directions in which the main beam takes a minimum value. The HPBW and FNBW are expressed as follow:

$$\text{HPBW} = |\theta_{\text{HPBWleft}} - \theta_{\text{HPBWright}}| \tag{3}$$

$$\text{FNBW} = |\theta_{\text{FNleft}} - \theta_{\text{FNright}}| \tag{4}$$
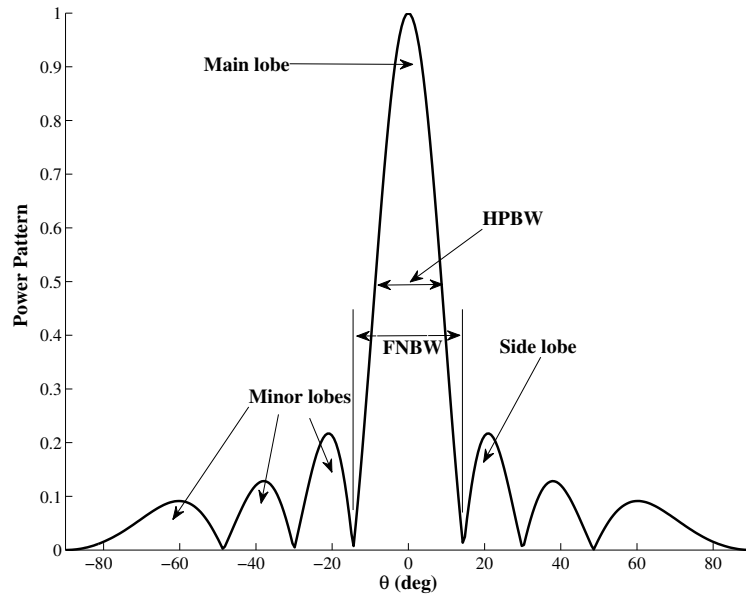
(a)
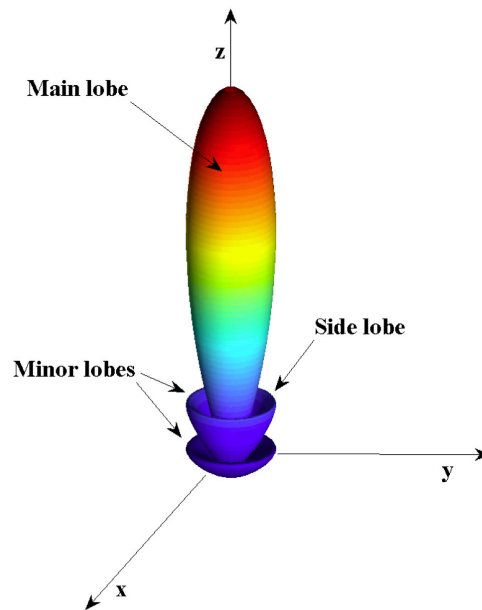
(b)

Figure 5. (a) Linear plot of power pattern and its associated lobes and beamwidths. (b) Radiation lobes of an antenna pattern (three dimensions).

where θ_{HPBWleft} and $\theta_{\text{HPBWright}}$ are points to left and right of the main beam maximum for which the normalized power pattern has a value of one-half. In (4), θ_{FNleft} and θ_{FNright} are the main beam nulls where the array factor first goes to zero. The beamwidth is an important figure of merit, and it often used to as trade-off between it and side lobe level. In addition, the beamwidth in antennas is also used to describe the resolution capabilities of the antenna to distinguish between two adjacent radiating sources or radar targets.

One important description of an antenna array is how much it concentrates energy in one direction in preference to radiation in other directions. This property of an antenna is called its directivity (D) and in mathematical form can be expressed as (Balanis, 1997):

$$\text{D}(\theta, \phi) = \frac{U(\theta, \phi)}{P_{\text{rad}}/4\pi} \qquad\qquad \text{D}(\theta, \phi)_{\text{max}} = \frac{U(\theta, \phi)_{\text{max}}}{P_{\text{rad}}/4\pi} \tag{5}$$

In (5), if the direction (θ, ϕ) is not specified, it implies the direction of maximum radiation intensity $\text{D}(\theta, \phi)_{\text{max}}$. In addition, the power radiated (P_{rad}) is the integral, in spherical coordinates, of the radiation intensity $U(\theta, \phi)$ in all directions of space,

$$P_{\text{rad}} = \int_0^{2\pi}\int_0^{\pi} U(\theta, \phi)\sin\theta\, d\theta\, d\phi \tag{6}$$

If the analysis is based on isotropic antennas, the radiation intensity is proportional to the square of the array factor,

$$U(\theta, \phi) \propto |\text{AF}(\theta, \phi)|^2 \tag{7}$$

Substuting (5), (6) and (7), the directivity is rewritten as:

$$D = 4\pi \frac{|\mathrm{AF_{max}}|^2}{\displaystyle\int_0^{2\pi}\!\!\int_0^{\pi} |\mathrm{AF}(\theta,\phi)|^2 \sin\,d\theta\,d\phi} = \frac{2|\mathrm{AF_{max}}|^2}{\displaystyle\int_0^{\pi} |\mathrm{AF}(\theta)|^2 \sin\,d\theta} \tag{8}$$

In (8), the double integral of the denominator represents the total radiated power and it can be simplified due to the dependence of AF on the spacing between antenna elements and the progressive phase shift.

2.2.2 Linear antenna arrays

The most common and most analyzed structure is the linear antenna array, which consists of antenna elements separated on a straight line by a given distance. If adjacent elements are equally spaced then the array is referred to as a uniform linear array (ULA). If in addition, the feeding amplitudes are constant, i.e. $I_n = I$, then this is known as a uniform array. Finally, if the phase $\alpha_n = n\alpha$, where α is a constant, then the array is a progressive phase shift array (Allen & Ghavami, 2005).

Assuming a linear array of N equally spaced elements (ULA) considering isotropic radiators as shown in Figure 6, the array factor is given by (Balanis, 1997):

$$\mathrm{AF} = I_0 + I_1 e^{jkd\cos\theta} + I_2 e^{jk2d\cos\theta} + \cdots + I_{N-1} e^{jk(N-1)d\cos\theta} = \sum_{n=0}^{N-1} I_n e^{jknd\cos\theta} \tag{9}$$
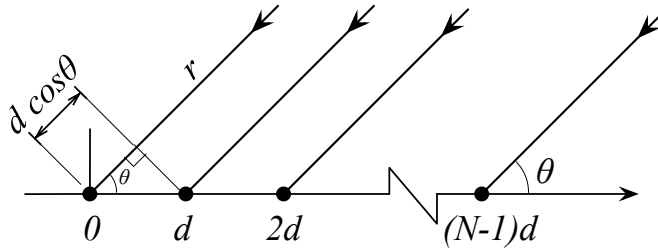
Figure 6. Equally spaced linear array of isotropic point sources.

where $I_0, I_1, ...$ are the excitation coefficients[11] with amplitude and phase shift, $k = 2\pi/\lambda$ is the wavenumber, d is the spacing between elements and θ is the angle in relation with the array axis. If the current has a linear phase progression (i.e., relative phase between adjacent elements is the same), the phase can be separated explicitly as:

$$I_n = A_n e^{jn\alpha} \tag{10}$$

here A_n and α are real coefficients, where the $(n+1)^{\text{th}}$ element leads the nth element in phase by α. Then (9) becomes

$$\text{AF}(\Psi) = \sum_{n=0}^{N-1} A_n e^{jn(kd\cos\theta+\alpha)} = \sum_{n=0}^{N-1} A_n e^{jn\Psi} \tag{11}$$

where the electric angle $\Psi = kd\cos\theta + \alpha$. This phase difference is equal to the sum of phase shift due to the path difference $(kd\cos\theta)$, plus the progressive phase α.

If the main beam is scanned considering the same linear array with equally spaced elements, (11) it can be rewritten as:

$$\text{AF}(\theta) = \sum_{n=0}^{N-1} A_n e^{j[knd(\cos\theta-\cos\theta_0)+\delta_n]} \tag{12}$$

Since $\alpha = -knd\cos\theta_0$ varies linearly with position term nd, it is referred to as linear phase, or uniform progressive phase. The remaining part of the excitation phase δ_n is nonlinear with distance and is useful in beam shaping.

---

[11]A complex number composed by amplitude and phase in a single entity.

2.2.3   Planar antenna arrays

In a planar o rectangular array the individual radiators can be positioned along a rectangular grid. Planar arrays provide additional variables which can be used to control and shape the pattern of the array. In contrast to linear array arrangement (which allows one to steer the beam into any direction in the azimuth plane), the planar antenna array allows one to steer the beam in elevation. In addition, this type of multidimensional arrays are more versatile and can provide more symmetrical patterns with lower side lobes (Mailloux, 1994).

The array factor for a planar array (rectangular lattice) $N \times M$ with equally spaced elements in the xy-plane (Figure 7), with spacing d_x in x direction, and d_y in y direction, where I_{mn} represents the current distribution. In analogy, with linear array antenna (9), the array factor of a planar array is (Balanis, 1997):

$$\text{AF} = \sum_{n=0}^{N-1} \sum_{m=0}^{M-1} I_{mn} e^{jm(kd_x \sin\theta \cos\phi)} e^{jn(kd_y \sin\theta \sin\phi)} \tag{13}$$

Considering a progressive phase excitation α_x in x direction and α_y in y direction as in (10):

$$I_{mn} = A_{mn} e^{jm\alpha_x} e^{jn\alpha_y} \tag{14}$$

And the array is rewritten as:

$$\text{AF} = \sum_{n=0}^{N-1} \sum_{m=0}^{M-1} A_{mn} e^{jm(kd_x \sin\theta \cos\phi + \alpha_x)} e^{jn(kd_y \sin\theta \sin\phi + \alpha_y)} \tag{15}$$

In the same way as in (11), considering again the array factor can be written in terms of the electric angle as:
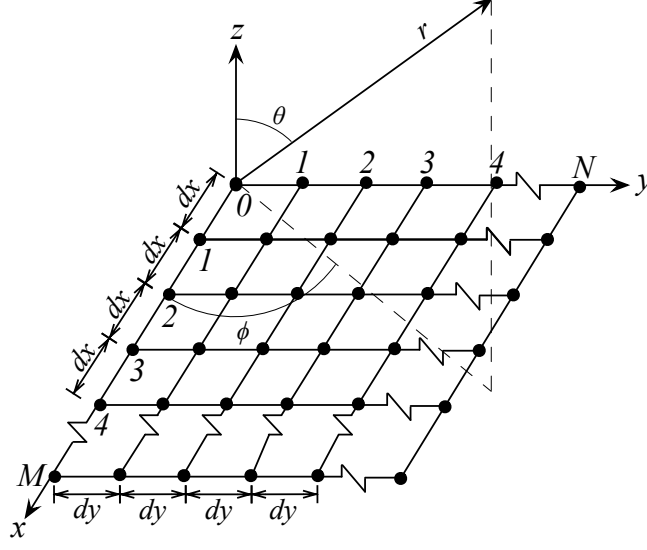
Figure 7. $N \times M$ rectangular planar array.

$$\text{AF}(\Psi_x, \Psi_y) = \sum_{n=0}^{N-1} \sum_{m=0}^{M-1} A_{mn} e^{jm\Psi_x} e^{jn\Psi_y} \qquad (16)$$

If exists the same amplitude excitation in rows parallel to the x-axis and identical amplitude excitation in all columns, in this case the amplitude excitation is separable (e.g., $A_{mn} = A_m A_n$) and (16) is written as:

$$\text{AF}(\Psi_x, \Psi_y) = \sum_{n=0}^{N-1} A_m e^{jm\Psi_x} \sum_{m=0}^{M-1} A_n e^{jn\Psi_y} \qquad (17)$$

Additionally, considering the scanning of the main beam (in the same way as in (12)) the array factor is written explicitly as:

$$\text{AF}(\theta, \phi) = \sum_{n=0}^{N-1} \sum_{m=0}^{M-1} A_{mn} e^{j[kmd_x(\sin\theta\cos\phi - \sin\theta_0\cos\phi_0) + knd_y(\sin\theta\sin\phi - \sin\theta_0\sin\phi_0) + \delta_{mn}]} \qquad (18)$$

where δ_{mn} represents the phase excitation of the mn^{th} element. This parameter is used as a design parameter in the array antenna synthesis.

2.3   The Antenna Pattern Synthesis Problem

Antenna synthesis in its broadest sense consists of specifying a desired radiation pattern and then using a systematic method (typically an analytical method) or combination of methods to arrive at an antenna array configuration that produces a pattern which approximates the desired pattern, as well as satisfying other system constraints. Unfortunately, there is no single synthesis method that yields the optimum antenna for the given system specifications.

Being more specific, the antenna pattern synthesis problem consists of determining the excitation of a given antenna type[12] that leads to a radiation pattern which suitably approximates a desired pattern (Stutzman & Thiele, 1998). The desired radiation pattern can vary widely depending on the application (e.g. satellite systems or radar systems) and has different variables, such as multiple beams, shaped beams, low side lobes, shaped side lobes, nulls and many others.

As mentioned earlier, there is no general method of synthesis. Instead, synthesis methods have been developed for each antenna type. Only a few deterministic methods can be used to a variety of antenna and pattern types (Stutzman & Coffey, 1975). Usually, deterministic methods for shaped beam patterns are completely different from those for low side-lobe, narrow beam patterns to name a few.

2.4   Metaheuristics as an Optimization Tool in the Antenna Design

On the other hand, stochastic algorithms for optimization can be considered a type

---

[12]This refers to the geometry of the antenna and consists of continuity, shape and size.

of general problem solver that can be applied to many difficult problems in different applications, including the antenna pattern synthesis (Jin & Rahmat-Samii, 2007; Karimkashi & Kishk, 2010; Rocca *et al.*, 2011; Weile & Michielssen, 1997).

As an alternative to the classic theories, stochastic optimization methods are becoming more important within the field of electromagnetic design[13]. These kind of stochastic algorithms usually involves metaheuristics[14]. A heuristic or metaheuristic finds quality solutions to a tough optimization problem in a reasonable amount of time, but there is no guarantee that optimal solutions are reached (Eiben & Smith, 2003). Most metaheuristic algorithms are nature-inspired as they have been developed based on some abstraction of nature.

In this way, metaheuristics are a powerful tool for designing antenna arrays and have been used extensively for this problem in recent years. In this work, two well-known population-based metaheuristics are studied: Genetic Algorithms (GA) (Holland, 1992; Goldberg, 1989) and Particle Swarm Optimization (PSO) (Kennedy & Eberhart, 1995; Kennedy *et al.*, 2001). These algorithms are briefly described below.

2.4.1 Genetic Algorithms

The genetic algorithms were developed by John Henry Holland and his collaborators in the 1960s and 1970s. GA is a model or abstraction of biological evolution and are based on Charles Darwin's theory of natural selection. Holland introduced the crossover or recombination, mutation, and selection in the study of adaptive and artificial systems. These genetic operators form the essential part of the genetic algorithm as a problem-

---

[13]Some references in this topic are: (Hoorfar, 2007; Karimkashi & Kishk, 2010; Rahmat-Samii *et al.*, 2012; Robinson & Rahmat-Samii, 2004; Rocca *et al.*, 2011; Weile & Michielssen, 1997).

[14]The "meta" prefix means beyond or higher level denoting a better performance than simple heuristics.

solving strategy (Holland, 1992; Eiben & Smith, 2003).

Genetic algorithms consider a population of chromosomes (individuals) encoding potential solutions to a given problem. Within the traditional GA model, the chromosomes are bit strings of a fixed length. Each chromosome represents a point in the search space. The search progress is obtained by recombination or modification of the chromosome population. To control the search progress, an evaluation of each chromosome is necessary with the aim to find a solution to the problem concerned. This evaluation is usually done by means of a quality (fitness) function (Goldberg, 1989; Eiben & Smith, 2003).

A basic procedure of the genetic algorithms is shown below:

- Encoding the objectives or optimization functions.
- Defining a fitness function or selection criterion.
- Initializing a population of individuals.
- Evaluating the fitness of all the individuals in the population.
- Creating a new population by performing crossover, mutation, fitness proportionate reproduction.
- Evolving the population until certain stopping criteria are met.
- Decoding the results to obtain the solution to the problem.

The steps of this basic procedure can be represented by a pseudo-code as shown in Algorithm 1.

Detailed information of terms and implementation of GA can be found in (Goldberg, 1989).

Algorithm 1 Pseudo-code of genetic algorithms

Encode the potential solutions into chromosomes
Objective function $f(x)$, $x = (x_1, ..., x_n)^T$
Define fitness
Generate initial population
Initial probabilities of crossover (P_c) and mutation (P_m)
Evaluate the fitness of the population
   while $t <$ Max number of generations **do**
   Generate new solution by crossover and mutation
     if $P_c > rand$ **then**
       Crossover
     end if
     if $P_m > rand$ **then**
       Mutate
     end if
Accept the new solutions if their fitness increase
Select the current best for new generation (elitism)
   end while
Decode the results and perform visualization

2.4.2   Particle Swarm Optimization

Particle swarm optimization (PSO) was developed by James Kennedy and Rusell C. Eberhart in 1995, based on the social behaviour exhibited by biological communities to satisfy their immediate needs, such as fish and bird schooling in nature (Kennedy & Eberhart, 1995; Engelbrecht, 2005).

PSO algorithm as an optimization tool offers valuable features such as the fact that each individual in the population has a basic type of memory, ease of implementation and small number of parameters to be selected and tuned in one operator (velocity), compared with other population-based methods, including genetic algorithms, where the memory concept relies on few individuals (elitism) and the parameters to be selected and tuned are related to multiple operators.

In PSO the set of parameters to be optimized define a particle or potential solution.

A collection of particles or individuals form the swarm (population) where each particle moves through one basic operator (velocity). In this way, the behavior of PSO can be summarized in the velocity operator $v_{ij}(t)$ and a position equation $x_i(t)$ respectively (Kennedy *et al.*, 2001), given by:

$$v_{ij}(t+1) = \omega v_{ij}(t) + c_1 r_{1j}(t)[y_{ij}(t) - x_{ij}(t)] + c_2 r_{2j}(t)[\hat{y}_j(t) - x_{ij}(t)] \tag{19}$$

$$x_{ij}(t+1) = x_{ij}(t) + v_{ij}(t+1) \tag{20}$$

where ω is the inertial weight that regulates the impact of previous velocities in the new particle velocity, $v_{ij}(t)$ is the velocity of particle i in dimension $j = 1, \ldots, n_x$ at time step t, $x_{ij}(t)$ is the position of particle i in dimension j at time step t, c_1 is the cognitive parameter that indicates the maximum influence of the best personal experience in the particle and c_2 is the social parameter, which indicates the maximum influence of social information on the new value of the particle, both are known as the acceleration constants. The terms represented by r are random numbers uniformly distributed in $U[0, 1]$. The current personal best and global best are represented by $y_{ij}(t)$ and $\hat{y}_j(t)$, respectively.

The personal best, y_i, related with particle i is the best position the particle has visited since the first time step. Considering a minimization problem, the personal best position at the next time step, $t + 1$, is calculated as:

$$y_i(t+1) = \begin{cases} y_i(t) & \text{if } f(x_i(t+1)) \geq f(y_i(t)) \\ x_i(t+1) & \text{if } f(x_i(t+1)) < f(y_i(t)) \end{cases} \tag{21}$$

where $f : \mathbb{R}^{n_x} \to \mathbb{R}$ is the fitness function.

The global best position, $\hat{y}(t)$, at the time step t, is defined as:

$$\hat{y}(t) \in \{y_0(t), \dots, y_{n_s}(t)\} | f(\hat{y}(t)) = \min\{f(y_0(t)), \dots, f(y_{n_s}(t))\} \qquad (22)$$

where n_s is the total number of particles in the swarm. Note that the definition in (22) states that $\hat{y}$ is the best position discovered by any of the particles so far and it is usually calculated as the best personal best position.

Detailed information of the terminology can be found in (Kennedy *et al.*, 2001; Engelbrecht, 2005), and the implementation steps of PSO algorithm are summarized in the pseudo-code shown below (Algorithm 2).

Algorithm 2 Pseudo-code of particle swarm optimization

Objective function $f(x)$, $x = (x_1, ..., x_n)^T$
Initialize locations x_{ij} and velocity v_{ij} of n particles
Find $\hat{y}_j$ from min $\{f(x_1), \dots, f(x_n)\}$ (at $t = 0$)
  while (criterion) **do**
    $t = t + 1$ (pseudo time or iteration counter)
    for loop over all n particles and all d dimensions **do**
      Generate new velocity $v_{ij}(t + 1)$ using equation (19)
      Calculate new locations $x_{ij}(t + 1)$ using (20)
      Evaluate objective functions at new locations $x_{ij}(t + 1)$
      Find the current best for each particle y_{ij} (21)
    end for
    Find the current global best $\hat{y}_j$ (22)
  end while
Output the final results y_{ij} and $\hat{y}_j$

2.5   Chapter Summary

The theoretical bases of antenna arrays including antenna parameters and specific geometries (linear and planar arrays) analyzed throughout this thesis were described in this chapter. Thus, in this part of the document are described important radiation parameters that characterize and quantify the behavior of the radiation pattern of an

antenna, such as the side lobe level, directivity and beamwidth (half-power beamwidth and beamwidth between first nulls). Furthermore, the theoretical study of antenna arrays is based on considering the antenna elements of the arrangement as isotropic point sources. And therefore, the response of the antenna arrays discussed here is modeled in terms of its array factor.

Moreover, it is presented an overview of the problem of the antenna pattern synthesis, where its solution is raised from an approach based on evolutionary optimization. In this context, at the final of the chapter are presented two population-based metaheuristics widely known and used in complex electromagnetic problems, with the intention to be used in the antenna synthesis.

3. Beam-forming Networks based on CORPS

3.1 Introduction

In recent years, research in the field of periodic structures has regained popularity in electromagnetic community due to the special electromagnetic features offered in different applications. In this context, the Antennas Group at UPNA[15] is one of the research group involved in the study of these structures reporting a series of new results in this open line of research.

The specific field of research which is the main goal in this thesis, is based on considering the feed system of an antenna array as a periodic structure and in the study of the coupling mechanism within these structures. The convergence between these aspects leads to the CORPS-BFN concept.

The study of CORPS-BFN is based on the introduction and development of new design methodologies of antenna systems based on CORPS and in the proposal of a new application area. In this way, the fundamentals of CORPS technology and the mathematical modeling for a CORPS-BFN are described in this chapter.

3.2 Definition and Radiation Features of CORPS

CORPS is defined by its creators as Coherently Radiating Periodic Structures. This acronym is based on the main features offered by these structures: coherent coupling, radiation (possible application of such structures) and periodic structures (Garcia *et al.*, 2005; Betancourt & del Rio Bocio, 2007).

---

[15]The acronym refers to the Public University of Navarra on Pamplona, Spain.

The behavior or working principles of coherently radiating periodic structures are based on the combination of different effects. One of the main effects is related to the coupling mechanism and its positive use controlling it. Therefore, the study of CORPS focuses on dealing with the coupling effect among elements of a periodic structure with the main idea of having total control of it. For the above, one can define an ideal coupling effect as lossless process in which the power is divided ideally through the periodic structure, i.e., when an element of the structure maintains the half of power and the remaining half of power is coupled to neighboring elements.

Formally a coherently radiating periodic structure is defined by three basic principles as follows (Betancourt & Rio, 2011):

1. First, the structure should allow the propagation of energy through it. Such energy propagation is designed to be lossless in one direction (e.g. z-axis) for a defined frequency band (see Figure 8).

2. The energy propagation inside the structure is limited. This process in which the energy propagation is carried inside the structure and no through it, is denoted as the spread of energy[16] inside the structure. The spread of energy can be performed throughout the structure or be confined to a specific area in the structure. For the specific case of a CORPS structure this spread of energy is confined. In this way, to control or limit the process of spread of energy inside of a CORPS structure, it is specified a spread control process (Figure 8) inside the structure. In this way, the spread control assure the propagation of energy through the structure by restricting the propagation of energy inside it.

3. The CORPS concept is based in the presence of intense coupling effects, such

---

[16]Term defined as the energy that flux inside the structure in the horizontal axis (x or y plane).

effects are designed to be coherent. Therefore, the coherent coupling is defined in a CORPS structure. This coherent coupling is referred to as in-phase feature contained in each element of a CORPS structure where the overall effect of each in-phase feature at each element over the periodic structure. The above, relate the coherent coupling with the capacity of a CORPS structure to overlap areas or regions without loss of information. This property is illustrated in Figure 8. In addition it should be noted that this coherent effect is responsible of the radiation characteristics of the structure allowing to carry out signals through it defining its multiple-beam features.
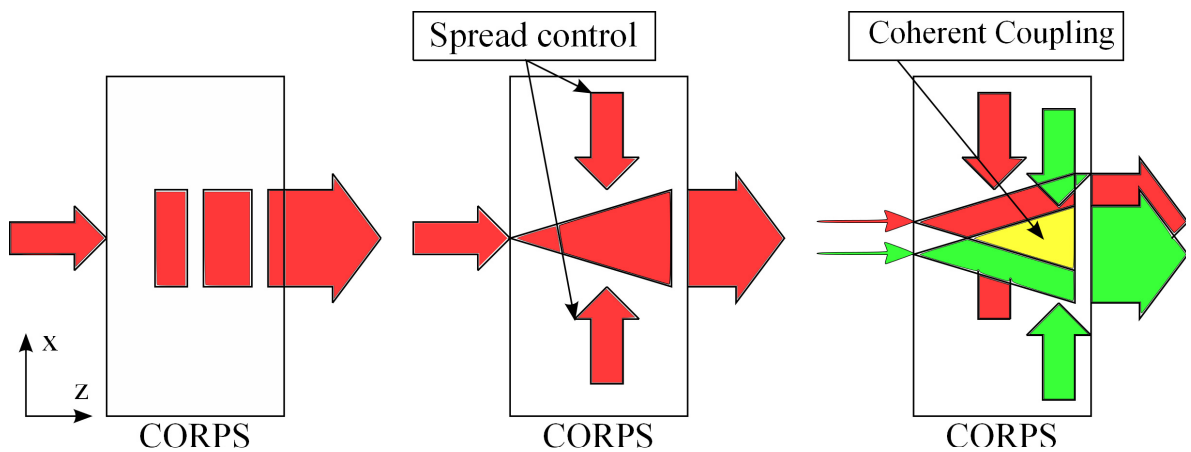
Figure 8. Schematic representation of the features of CORPS structures, the propagation of energy throughout the structure (left structure), the spread control (center structure) and the coherent coupling mechanism (right structure).

The existence of a CORPS structure strictly obeys the three basic principles presented above, which must be always present at same time.

From the effects described above, concerning the ideal coupling, the spread control and the coherent coupling; a schematic representation of a single and isolated element of a CORPS structure is shown in Figure 9. The objective of Figure 9 is to clarify the behavior of these properties on a single element. The CORPS element represents a black

32

box composed by three outputs and one input. The side output ports are bidirectional ports to manage the power in adjacent elements as a part of spread control and ideal coupling behavior. The output port located in the center is the no coupling output. Additionally, it should be noted that the coherent coupling in the structure element is also present and described as a property to deliver in-phase signals to every output port.
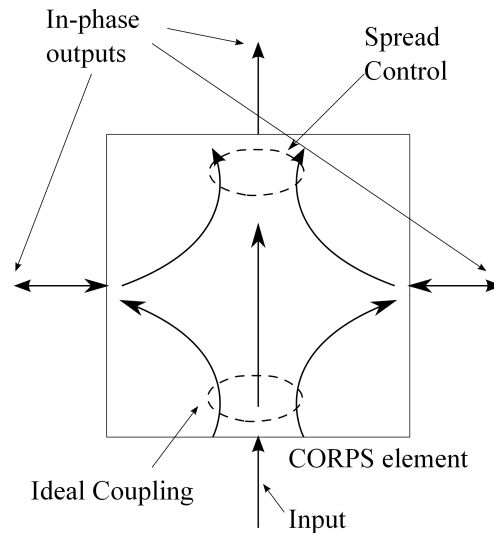
Figure 9. Schematic figure of a CORPS element illustrating its properties.

A complete scheme of a CORPS system formed by N black-box elements is shown in Figure 10. The objective is to illustrate the effects previously studied at system level. In this network two signals (color red and green) excite the network, showing the behavior of the signal propagating (propagation of energy) through the structure between layers. The propagation inside the structure is limited resulting in a defined path (spread control). The second excitation (green signal) have the same behavior as the red path for the energy propagation, sharing the same path after some layers until the end of the network.

In this periodic structure where exists an interconnection symmetry between ele-
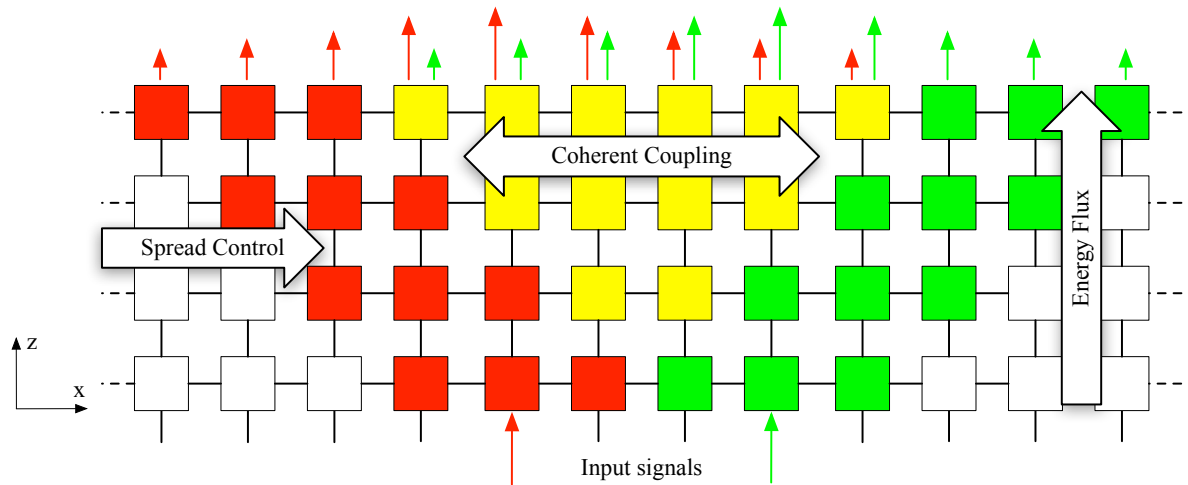
Figure 10. Schematic illustration of a CORPS structure and its effects.

ments, the electromagnetic fields carrying information are combined without loss of information (Betancourt & Rio, 2011). Thus the effect known as coherent coupling, allows to share the same resources into the periodic structure (in this case, the same path) for different information signals without loss of information. The above, is reflected in the schematic as the combination of both colors (red and green), resulting in a yellow color (based in a RGB[17] color model) and demonstrating that effects such as coherent coupling and spread control can be used to carry multiple information signals at same time. The difference with introducing a new signal or beam is that its phase center is displaced depending on the input port used. The result of such behavior in a CORPS network are the capabilities to overlapping of multiple beams and to generate high angular resolution system.

---

[17]This abbreviation refers to the RGB additive color model in which red, green, and blue light are added together in different ways to reproduce a broad palette of colors.

3.3 CORPS as a Beam-forming Network

Based on Figure 10, representing a CORPS structure composed by N black boxes, the main features and behavior related to a beam-forming network based on CORPS principles were defined. The mathematical modelling of CORPS-BFN can be accomplished reducing the complexity of the black-box model illustrated in Figure 10. To simplify the complex black-box model dealing with ideal coupling and the spread control at the same time, it is used a schematic representation for a CORPS-BFN based on two different types of fundamental blocks (Betancourt & del Rio Bocio, 2007). The new schematic is shown in Figure 11.
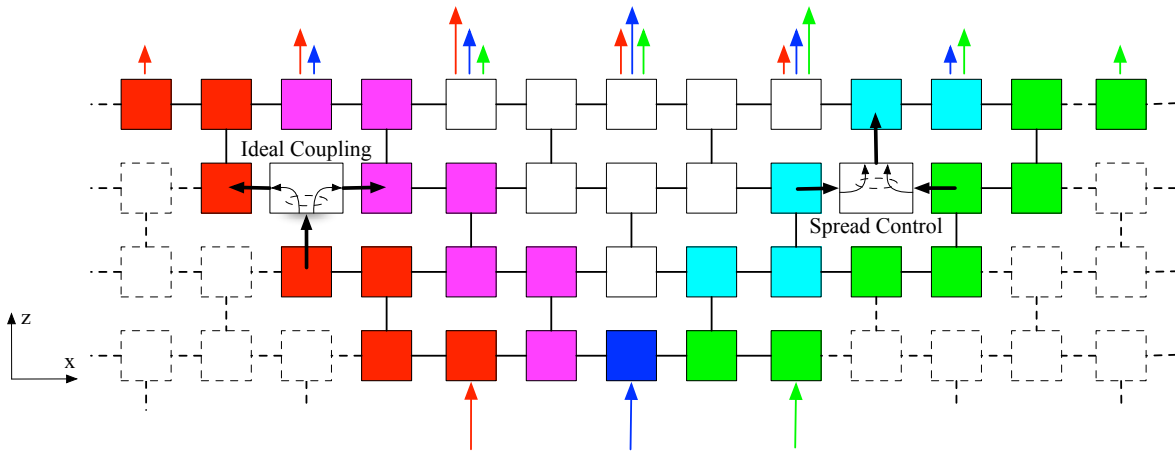
Figure 11. Schematic diagram of a CORPS system using simplified black boxes. The structure is excited with three different signals (red, blue and green), combined according the RGB color model and CORPS principles. Insets in figure shown the internal behavior of black boxes.

The basic blocks or nodes perform two specific tasks, one of them is responsible of the division of power and the other is in charge of the power combination. The block acting as a power divider is denoted as split node (S-node) and the power combiner block is denoted as recombination node (R-node). The S-node takes the signal in its input port and delivers the half of power by each of its output ports. On the other

hand, the R-node takes the signal present in its inputs (two input ports are considered) and deliver the combination of both for a single output. This new simplified model takes into account just three ports for the black boxes, rather the four for the basic blocks reducing the element complexity. The schematic in Figure 11, seeks to maintain the same behavior and similar propagation scheme as the schematic representation of the original model (Figure 10).

3.3.1   CORPS-BFN model

CORPS-BFN model considers the basic behavior principles of the periodic structures called CORPS (Garcia *et al.*, 2005) (Section 3.2), such model can be implemented using identical basic nodes or unit cells (Betancourt & del Rio Bocio, 2007). In this way, a CORPS network is formed by alternating iteratively split (S) and recombination (R) nodes, just changing its relative position as shown in Figure 12.

To model the behavior of this structure considering the characteristics of general split and recombination blocks, it must be taken into account the conservation of energy based in that a CORPS-BFN is formed only on lossless passive components.

If general-split nodes are such that have one input port and N output ports. The power introduced at input port is divided, a Nth part of the power is delivered at each output port, as follows (Betancourt & del Rio Bocio, 2007):

$$W_S = \sum_{k=1}^{N} |E_k e^{(j\theta_k)}|^2 G_S \tag{23}$$

where W_S is the power delivered by the N output ports in the split node, G_S is the real part of the admittance seen at output ports, E_k and θ_k with $k = 1, 2, ...N$ are the field magnitude and phase of each of the k output ports, respectively. For the S-node
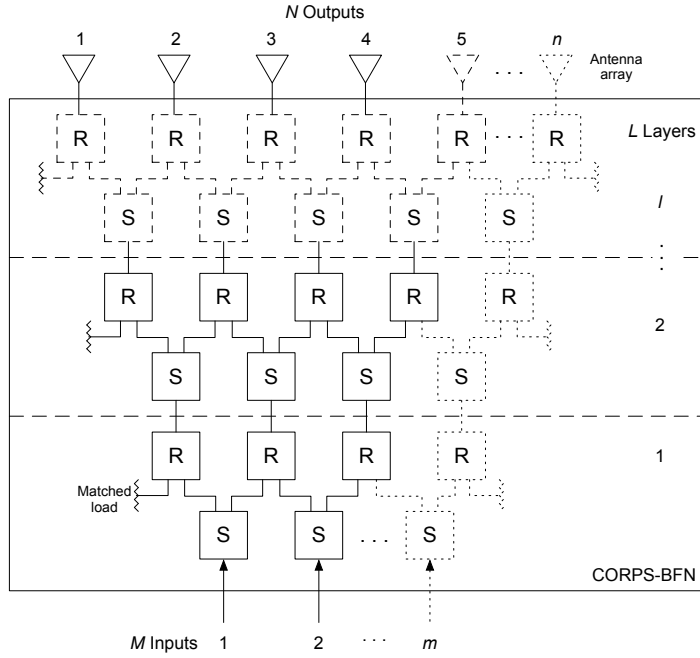
Figure 12. Schematic of a CORPS beam-forming network with S and R nodes of M inputs, N outputs and L layers.

analyzed and represented in Figure 12, where $N = 2$, (23) can be rewritten as:

$$W_S = (E_1^2 + E_2^2)G_S \tag{24}$$

For the case of general-recombination nodes that posses one output port and several sets of two input ports, the power (W_R) at the output port is given by:

$$W_R = \sum_{k=1}^{N} |E_{k,1}e^{(j\theta_{k,1})} + E_{k,2}e^{(j\theta_{k,2})}|^2 G_k \tag{25}$$

where E_k and θ_k with $k = 1, 2, ...N$ are the magnitude and phase of each set of input ports, respectively, and G_k is the admittance at the output. Rewritting (25) for a R-node of 1 set of input ports:

$$W_R = (E_{1,1}^2 + E_{1,2}^2 + 2E_{1,1}E_{1,2}\cos(\theta_{1,1} - \theta_{1,2}))G_R \tag{26}$$

Here, G_R is the admittance at the output. The last term with angles used in (26) defines the correlation between input fields at R-node based on its arrival phase. A vectorial summation of field vectors at input ports of R-node is applied for the phase calculus. For the S-node case, maintains the same phase shift from the input until the output.

Furthermore, it has been demonstrated that the behavior for power values after each layer correspond with Pascal's Triangle normalized by the sum of its in-row coefficients (Betancourt & del Rio Bocio, 2007). Consequently, in a CORPS-BFN of l layers, the amplitude at the $k+1$ output ports will have binomial shape.

In the same way, the output of a CORPS-BFN always has the same shape and phase distribution, independently of the number of layers used. In this manner, the amplitude distribution at the output ports of a CORPS-BFN will resemble a Gaussian distribution and the phase distribution will be expressed as a linear representation of phase shift set at input ports of the network.

A fundamental part in the analysis of CORPS-BFN is to describe the behavior of the network based on the black box properties of the basic nodes, i.e., S and R nodes. To perform the previous task, a basic node can be characterized as a 3-port component (used for power combination and power division) by the following scattering matrix[18] (Betancourt & del Rio Bocio, 2007):

$$[S]_{cell} = \frac{j}{\sqrt{2}} \begin{bmatrix} 0 & 1 & 1 \\ 1 & 0 & 0 \\ 1 & 0 & 0 \end{bmatrix} \tag{27}$$

The matrix is obtained using (24) and (26) and represents the behavior of an S-node

---

[18]Often referred to as Wilkinson's matrix.

38

or R-node. Furthermore, the ideal matrix in (27), ensures that the basic component is perfectly matched and isolated, and therefore there is no interaction between input signals. Therefore, S and R nodes in Figure 12 can be replaced with the scattering matrix in (27) to obtain a simulation model of a CORPS network.

A feed network based in CORPS composed by basic nodes (S or R nodes) is physically implemented replicating this basic constituting components for example by mean of a Gysel Power Divider[19] (Betancourt & del Rio Bocio, 2007) or by a Circular In-phase Hybrid Ring Power Divider (CIHRPD)[20] (Ferrando & Fonseca, 2011).

In order to calculate the fields at the output of each unit cell (S or R node) $[V^-]_{cell} = [V_1^- V_2^- V_3^-]^T$, the next equation can be used:

$$
\begin{bmatrix} V_1^- \\ V_2^- \\ V_3^- \end{bmatrix}_{cell} = \begin{bmatrix} S_{11} & S_{12} & S_{13} \\ S_{21} & S_{22} & S_{23} \\ S_{31} & S_{32} & S_{33} \end{bmatrix}_{cell} \cdot \begin{bmatrix} V_1^+ \\ V_2^+ \\ V_3^+ \end{bmatrix}_{cell} \tag{28}
$$

where $[S]_{cell} = [S_{11} \cdots S_{33}]^T$ is the scattering matrix of a unit cell and $[V^+]_{cell} = [V_1^+ V_2^+ V_3^+]^T$ is the complex excitation (amplitude and phase) at the input ports of a unit cell. Evaluating (28) and interconnecting a feed network as in Figure 12, it can be simulated and analyzed a beam-forming network that uses CORPS technology.

3.3.2 2D CORPS-BFN

Based on (Betancourt & Rio, 2011) and (Betancourt & del Rio Bocio, 2007), a general methodology to define a BFN based on CORPS is described. This methodology takes into account all possible configurations allowed to feed a N by N planar array. In the

---

[19]A$3\lambda/2$ ring impedance transformer of five ports.
[20]Hybrid ring with some improvements in terms of adaptation, isolation levels and wideband performances.

same way, this process divide into two stages the structure of a CORPS-BFN system to feed a rectangular planar array.

In order to standardize the terminology with literature (Betancourt & del Rio Bocio, 2007), the term CORPS-BFN of one dimension will be termed as C-BFN. These C-BFNs integrate a CORPS-BFN system (2D CORPS-BFN).

The CORPS feed network system is defined in two stages. Suppose that the first stage is composed by Q C-BFN that support the $Q \times M$ input ports of the system and the second stage contains N C-BFN to support the $N \times N$ output ports.

The design methodology and related parameters (i.e., N, M and Q) of a CORPS-BFN system is illustrated in Figure 13. The methodology is summarized in the following steps:
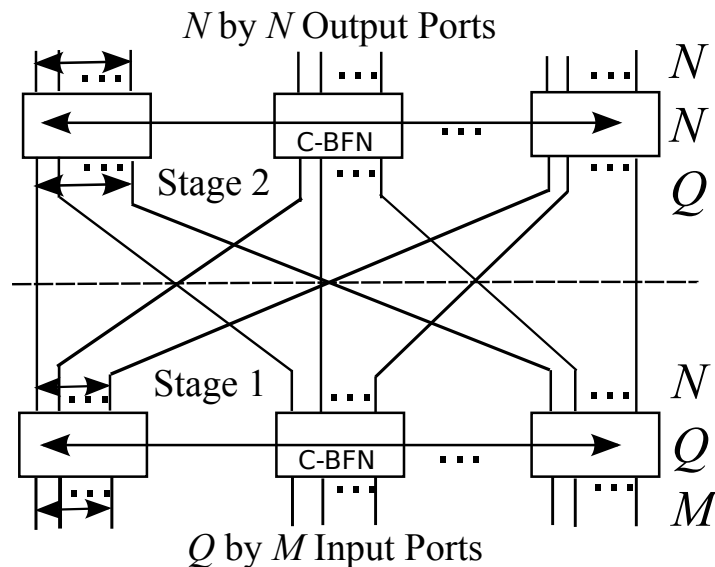
Figure 13. General scheme of a CORPS feed network system.

- Define the number of inputs/outputs of the feed system. Set $M \times M$ inputs and $N \times N$ outputs. Tipically $M \leq N$.

- Divide M into Q blocks. In this case, Q defines both the number of C-BFN blocks in stage 1 and the number of inputs of each block at stage 2. Tipically $Q \leq N$.

- Set the first stage with Q blocks (C-BFN) each one of M inputs and N outputs.

- Set the second stage with N blocks (C-BFN) each one of Q inputs and N outputs.

- Interconnect the first stage with second stage. The interconnection process between stages is carried out on the basis that each output of the first C-BFN at stage 1 (most left-one) is connected to the first input port of each C-BFN at second stage, and so forth.

In this way, a C-BFN of first stage is composed of $N - M$ layers and one in the second stage have $N - Q$ layers.

3.4 Chapter Summary

The fundamentals and working principles of CORPS technology are described in this chapter. The principles describing the coupling mechanisms within these structures define and give meaning to a CORPS structure. Similarly, this chapter includes the application of CORPS technology to beam-forming networks, which is the focus of this thesis. Thus, the CORPS-BFN is modeled mathematically from its basic unit (S or R node) which is used to form a complete network. Moreover, the CORPS-BFN is extended to bidimensional networks, through a detailed design methodology. Thus, this chapter in which the CORPS-BFN is modeled complements the foundations necessary to implement a complete antenna system, with its integration to the previous chapter concerning to the antenna array subsystem and the antenna pattern synthesis.

4. Design of Beam-forming Networks for Multi-beam Antenna Arrays based on CORPS: Part I - Mathematical Modeling

4.1 Introduction

The increase of technologies that require advanced features in modern antenna systems such as the dynamic redirection and reorganization of its services combined with the ability to handle multiple independent beams, require solutions that combine these characteristics efficiently. These features are combined effectively in multiple-beam forming networks (M-BFN).

There are different alternatives to use a M-BFN (as noted in Subsection 1.2). This chapter presents the technological concept of coherently radiating periodic structures applied into BFN (previously seen in Chapter 3) in order to design a multiple-beam forming network. In this way, CORPS-BFN technology is approached as as an alternative beam-forming network, efficient and innovative for multi-beam antenna systems.

In addition, an open research area in modern antenna systems is associated with the reduction and simplification the beam-forming network for the purpose of reducing weight, size and cost of a complete antenna system. In this context, the study of new structures for designing CORPS-BFN can be focused on design cases where the simplification and performance of the network can be improved for the antenna geometry and by advanced compression techniques used in the synthesis of antennas.

For the above, in this chapter three design approaches based on CORPS beam-forming networks are presented. The first two approaches are focused in the array

geometry (linear and planar antenna array, respectively) and the third one is based on the simplification of a CORPS-BFN using compressive arrays. In this way, the design of CORPS networks for antenna arrays is presented and divided into two chapters. This first part (Chapter 4) deals only with the mathematical modeling of these approaches and the second part (Chapter 5) with simulation case studies for each design approach.

4.2 Design Approach of a CORPS-BFN for Multi-beam Linear Antenna Array

The design of a beam-forming network for a steerable multi-beam antenna array in a linear geometry using the CORPS technology is presented. In this design, the input ports of the feed network are optimized using particle swarm optimization (PSO) algorithm (Section 2.4.2). In addition, the design strategy satisfies one of the most important trade-off related to the side lobe level (SLL) and directivity (D) (Section 2.2.1).

4.2.1 CORPS-BFN in linear arrays

To design a CORPS-BFN for an antenna array configuration, first it must be considered the CORPS-BFN model previously introduced in Section 3.3.1. This model is implemented using identical unit cells as a basic node (S or R nodes) to form an entire feed network, as was previously shown in Figure 12.

In this case, a unit cell is represented as a 3-port component characterized by the following scattering matrix, from (27) is written as:

$$[S]_{node} = \begin{bmatrix} 0 & \frac{j}{\sqrt{2}} & \frac{j}{\sqrt{2}} \\ \frac{j}{\sqrt{2}} & 0 & 0 \\ \frac{j}{\sqrt{2}} & 0 & 0 \end{bmatrix} \tag{29}$$

In the same way, in order to evaluate the fields (V^-) after an S-node or R-node, (28) can be simplified as follows:

$$V^- = SV^+ \tag{30}$$

In (30), S is the scattering matrix of a unit cell and V^+ is the complex excitation at the input ports of this unit cell. Using (30) and the schematic of a CORPS-BFN from Figure 12, it is possible to establish an iterative code that represents the propagation of signal throughout a CORPS-BFN configuration previously established.

Additionally, in the design of a CORPS-BFN it must be considered the geometry used on the antenna array. In this case, for linear arrays (one-dimensional) configurations it should be analyzed its array factor. Assuming an equidistant linear array, the array factor can be rewritten from (9) as follows:

$$\mathrm{AF}(\theta, \mathbf{a}, \mathbf{p}) = \sum_{n=1}^{N} I_n e^{jkd_n \cos\theta} \tag{31}$$

where I_n represents a complex excitation ($I_n = A_n e^{\xi_n}$) in the nth radiator of the array, k is the wavenumber, d_n represents the position of the nth antenna element with respect to the first radiator in the array and θ is the angle with respect to the normal that indicates the direction of radiation in the space.

The complex excitations feeding the M input ports of the CORPS network consider proposed inputs (i.e., the complex excitations to feed the nth radiator of the array) and

a progressive phase excitation (considering the feed network) and can be expressed as:

$$a_i = A_i \exp(j\xi_i) \exp(j\psi_i) \qquad \text{for} \quad 1 \leq i \leq N - L \qquad (32)$$

where N is the total number of antenna elements and L is the number of layers of the CORPS network. The term ψ_i in (32) is:

$$\psi_i = -kdm_i \cos\theta_0 \qquad (33)$$

In (33) θ_0 indicates the direction of maximum radiation and the parameter dm_i is given by:

$$dm_i = d_i + \frac{N-1}{N-1-L} \qquad (34)$$

here dm_i is not a design parameter. The idea of setting these parameters is the following: the first term $A_i \exp(j\xi_i)$ in (32) denotes the typical complex excitation (amplitude and phase, respectively) where $\xi_i \in [0, 180]$. The purpose of establishing this phase excitation is that the optimization process searches possible phase perturbations that generate a near-optimal array factor with angles of the main beam near the direction of interest. The second term $\exp(j\psi_i)$ adds a phase excitation in the complex inputs of the feed network related to a linear interpolation of a conventional progressive phase excitation.

Moreover, in the design of CORPS-BFN is necessary to confront the beam shaping. In this case, the antenna pattern synthesis is done with the help of evolutionary optimization. The reason for using this approach, is due to the number of possible input combinations to find a set of complex excitations that result in a radiation pattern that

meets specific objectives. This problematic could represent an NP-Hard[21] problem. For this reason population-based stochastic optimization algorithms are suggested with the benefit to handle multimodal and nonlinear optimization problems (Eiben & Smith, 2003).

The optimization process followed to obtain near-optimal solutions to the complex inputs to feed the BFN is described in the next subsection.

4.2.2 Optimization process using PSO

The optimization process in CORPS-BFN is used to obtain complex excitations (amplitudes and phases) that should be directly applied at the input ports of the network. For this specific case, these excitations are determined by a population-based metaheuristic called particle swarm optimization (PSO) (see Section 2.4.2).

The behavior of PSO can be summarized into a single operator (velocity) v_{kd}^t and an equation for the particle position x_{kd}^t, these equations can be rewritten from (19) and (20), respectively as follows:

$$v_{kd}^t = \omega v_{kd}^{t-1} + c_1 \varepsilon_{1k}(p_{kd}^* - x_{kd}^{t-1}) + c_2 \varepsilon_{2k}(g_d^* - x_{kd}^{t-1}) \quad v_{kd}^t \leq v_{d,max} \quad \forall d \qquad (35)$$

$$x_{kd}^t = x_{kd}^{t-1} + v_{kd}^t \qquad (36)$$

where ω is the inertial weight, c_1 and c_2 are the acceleration constants. The terms denoted by ε are random numbers uniformly distributed in $U[0, 1]$. The personal best and global best are denoted by p_{kd}^* and g_d^*, respectively.

The optimization process used by PSO follows the next steps: PSO generates particles as possible solutions. These particles or individuals are encoded by two vec-

---

[21]Nondeterminial polynomial-time hard.

tors of real numbers which represent amplitude $\mathbf{a} = [A_1, A_2, \ldots, A_{N-L}]^{22}$ and phase $\mathbf{p} = [\xi_1, \xi_2, \ldots, \xi_{N-L}]^{23}$ perturbations (A and ξ are the optimization variables proposed in the design procedure and each variable is treated separately). Each particle generates an array factor of certain characteristics of side lobe level and directivity. Then the PSO operator of velocity (35) and the position equation (36) are used for moving each particle through the solution space. Finally, PSO finds a global solution that generates an array factor with minimum side lobe level and maximum directivity in the desired direction.

In this work, PSO is used just as an optimization tool for the advantages of the algorithm itself. The performance comparison between PSO and other algorithms for this purpose is out of the scope of this research work.

The objective function can be deduced using (2) and (8), and can be written as:

$$
\begin{aligned}
minimize \quad & (|\mathrm{AF}(\theta_{\mathrm{SLL}}, \mathbf{a}, \mathbf{p})| / \max |\mathrm{AF}(\theta, \mathbf{a}, \mathbf{p})|) + (1/\mathrm{D}(\theta, \mathbf{a}, \mathbf{p})) \\
subject\ to \quad & A_i \in \mathbb{A} \ \text{and} \ \xi_i \in \mathbb{P}, \quad \forall i = 1, 2, \ldots, N - L
\end{aligned}
\tag{37}
$$

where $\mathbb{A} = [4, 12]$ and $\mathbb{P} = [0, 180]$ are the amplitude and phase domains, respectively, and θ_{SLL} is the angle where the maximum side lobe is attained. The goal is to minimize the weighted sum that involves both objectives (side lobe level and directivity respectively), which are uniformly weighted in the cost function.

---

[22]A_{N-L} represents the amplitude excitation of the $(N - L)^{\mathrm{th}}$ input port of the CORPS network in the set $\mathbf{a}$.

[23]ξ_{N-L} represents the phase excitation of the $(N - L)^{\mathrm{th}}$ input port of the CORPS network in the set $\mathbf{p}$.

4.3 Design Approach of a CORPS-BFN for a Multi-beam Planar Antenna Array

This design approach deals with a novel way to design and analyze beam-forming networks for a steerable multi-beam planar antenna array using CORPS structures. The complex inputs of the feed network are optimized using the well-know method of Genetic Algorithms (GA)(Section 2.4.1). The main objective of this approach is presenting a new perspective in the design of a CORPS-BFN considering a scannable multi-beam planar array with optimized inputs.

4.3.1 CORPS-BFN in planar arrays

Similarly to the linear case, the CORPS-BFN design for a planar antenna array configuration is based in the CORPS-BFN model presented in Section 3.3.1. Therefore, it is necessary to represent a basic node as in (29) and use (30) to determine the fields at the output of each node. In the same way, it is necessary to define a configuration based on Figure 12 to establish initially configurations in one dimension.

At the top of the feed network, it must consider the geometry used on the antenna array. In this case it is assumed an equidistant planar array of $N \times N$ antenna elements (two-dimensional). For simplicity, consider the planar array to be made of omnidirectional antenna elements. Its array factor can be extracted from (13) and is rewritten in the next equation:

$$\text{AF}(\theta, \varphi, \mathbf{a}, \mathbf{p}) = \sum_{i=1}^{N} \sum_{j=1}^{N} I_{ij} e^{jk[(x_{ij} \sin\theta \cos\varphi) + (y_{ij} \sin\theta \sin\varphi)]} \tag{38}$$

where I_{ij} represents the complex excitation ($I_{ij} = A_{ij} e^{\xi_{ij}}$) of the ij^{th} antenna element of the array, k is the wavenumber, x_{ij} and y_{ij} indicate the position of the ij^{th} element

of the array and the angles θ and φ indicate the spatial direction of radiation in the elevation and azimuth plane respectively.

The complex excitations feeding the M input ports of the CORPS-BFN system consider the proposed inputs (i.e., the complex excitation to feed the ij^{th} radiator of the array) and a progressive phase excitation (considering the feed network) and are given by:

$$a_{ij} = A_{ij} \exp(j\xi_{ij}) \exp(j\psi_{ij}) \qquad \text{for} \quad 1 \le i \le M \quad \text{and} \quad 1 \le j \le M \qquad (39)$$

where M represents the number of input ports of each C-BFN that electronically control the radiation pattern ($M = N - L$). The term ψ_{ij} in (39) is:

$$\psi_{ij} = -k[xm_{ij} \sin\theta_0 \sin\varphi_0 + ym_{ij} \sin\theta_0 \cos\varphi_0] \qquad (40)$$

In (40), (θ_0, φ_0) indicate the direction of maximum radiation in azimuth and elevation respectively and the parameters xm_{ij} and ym_{ij} are given by:

$$xm_{ij} = x_{ij} + (d/L)(i-1) \qquad ym_{ij} = y_{ij} \cos(\theta/L) \qquad (41)$$

where d is the constant value of uniform spacing between antenna elements in the array and L is the total number of layers of the CORPS-BFN system. Similarly to the linear case, xm_{ij} and ym_{ij} are not design parameters. Basically the idea of setting these parameters are the same as in the linear case. The first term $A_{ij} \exp(j\xi_{ij})$ in (39) denotes the typical complex excitation (amplitude and phase, respectively) where $\xi_{ij} \in [0, 180]$. The second term $\exp(j\psi_{ij})$ adds a phase excitation in the complex inputs of the feed network related to a linear interpolation of a conventional progressive phase

excitation.

In this case, a similar optimization process as described in Section 4.2.2 is used and is presented in the next subsection.

4.3.2 Optimization process using GA

The optimization process in CORPS-BFN is used to obtain complex excitations (amplitudes and phases) that should be directly applied at the input ports of the network. For a bidimensional feed network, this task can be considered more complex since several one-dimensional CORPS-BFN blocks have to be fed and interconnected. The steps for the interconnection of CORPS-BFN blocks are described in the methodology presented in Section 3.3.2.

To feed a planar antenna array, it was selected a robust and well-known heuristic technique called genetic algorithms (GA) (see Section 2.4.1).

By analogy with the process of natural selection and evolution, in GA the set of parameters to be optimized (genes) defines an individual or potential solution X (chromosome). A collection of individuals form the population, which evolves through three basic operators (selection, crossover and mutation). The optimization process used by the GA follows the next steps: The genetic algorithm generates individuals as candidate solutions. These individuals are encoded in two vectors of real numbers which represent amplitude $\mathbf{a} = [A_1, A_2, \ldots, A_{N-L}]$ and phase $\mathbf{p} = [\xi_1, \xi_2, \ldots, \xi_{N-L}]$ perturbations (A and ξ are the optimization variables proposed in the design procedure and each variable is treated separately). Each individual generates an array factor of certain characteristics of side lobe level and directvity. Then, the genetic operators of selection, crossover, and mutation are used to obtain solutions which tend to improve with each iteration.

The genetic algorithm evolves the individuals to a global solution that generates an array factor with minimum side lobe level and maximum directivity in the direction of interest.

In this work, in the same manner as PSO the genetic algorithm is used just like an optimization tool for the advantages of the algorithm itself, performance evaluation between GA with others algorithms in this application is outside the scope of this thesis.

Finally, the objective function to minimize can be written as:

$$
\begin{aligned}
&minimize \quad (|\mathrm{AF}(\theta_{\mathrm{SLL}}, \varphi_{\mathrm{SLL}}, \mathbf{a}, \mathbf{p})| / \max |\mathrm{AF}(\theta, \varphi, \mathbf{a}, \mathbf{p})|) + (1/\mathrm{D}(\theta, \varphi, \mathbf{a}, \mathbf{p})) \\
&subject\ to \quad A_i \in \mathbb{A} \ \text{and} \ \xi_i \in \mathbb{P}, \quad \forall i = 1, 2, \ldots, N - L
\end{aligned}
\tag{42}
$$

where $\mathbb{A} = [1, 14]$ and $\mathbb{P} = [0, 180]$ are the amplitude and phase domains, respectively, and $(\theta_{\mathrm{SLL}}, \varphi_{\mathrm{SLL}})$ is the angle where the maximum side lobe is attained. The goal is to minimize the trade-off between both objectives (side lobe level and directivity) that are uniformly weighted in the cost function.

4.4 Design Approach in the Simplification of a CORPS-BFN using the Matrix Pencil Method

In this section an innovative way to simplify the design of beam-forming networks based on CORPS technology for steerable multi-beam antenna arrays using the non-iterative matrix pencil method (MPM) is presented. This design approach is based on the application of the MPM in linear arrays fed by CORPS-BFN configurations to further reduce the complexity of the beam-forming network. In this manner, the objective of this approach is to demonstrate the possible simplification of a CORPS-BFN applying the MPM to the antenna array to reduce the number of the antenna

elements, but generating an approximate radiation pattern with a less complex BFN design.

4.4.1   The CORPS-BFN subsystem and its optimization

The first step in this design approach considering the linear case, is to take into account the CORPS-BFN model previously presented in Section 3.3.1. And then, follow the steps that are exactly the same as for the design approach for a linear antenna array previously presented in this chapter, in Section 4.2. This can be done by replicating the explained process from (29) to (34).

In the same way that all the above approaches discussed in this work. The next step is to apply an optimization process to obtain the complex excitations that should be applied at the input ports of the network, in this specific case the PSO algorithm is applied in the same manner as in Section 4.2.2. Finally, it is necessary to apply the method to reduce the number of antenna elements of the linear array while maintaining a similar radiation pattern. This method is explained in the next subsection.

4.4.2   The matrix pencil method applied to the compression of the antenna array

In order to compress a one-dimensional antenna array of M elements using the Matrix Pencil Method developed by Liu *et al.* (2008), (31) can be parameterized in terms of u (reference pattern) for sampling purposes, as follows:

$$\text{AF}_{\text{ref}}(u) = \sum_{n=1}^{M} I_n e^{jkd_n u} \tag{43}$$

where $u = \cos\theta$, and must be resolved the following optimization problem:

$$minimize \quad (P)$$

$$subject\ to \quad \left\{ \min_{\{I_n^*, d_n^*\}_{n=1,\dots,P}} \left\| \mathrm{AF}_{\mathrm{ref}}(u) - \sum_{n=1}^{P} I_n^* e^{jkd_n^* u} \right\|_L \right\} \leq \epsilon \tag{44}$$

where I_n^* and d_n^* $\forall n = 1, \dots, P$ are the complex excitation and the position of the P antenna elements obtained after the compression. Additionally, if the least square error (LSE) is used, then $L = 2$. If the LSE is less than ϵ, then the new one-dimensional array has the minimum number of elements while maintaining the same radiation pattern as the reference array factor $\mathrm{AF}_{\mathrm{ref}}(u)$. The methodology for solving this problem consists of two stages, in the first one is computed the singular value decomposition (SVD) of the Hankel matrix $[\mathbf{Y}]$ formed by the S samples of the parameter u in the reference array factor $\mathrm{AF}_{\mathrm{ref}}(u_s)$. That is, $\forall u_s = s\Delta = s/S$, $s = -S, \dots, 0, \dots, S$ subject to the Nyquist sampling theorem condition $\Delta \leq \lambda/2d_{\max}$, where $d_{\max} = \max\{d_n\}$. In this way, it is obtained the spectrum of the E singular values which determines the elements to be discriminated in the calculation of the array factor according to the following expression:

$$P = \min \left\{ p; \left| \frac{\sqrt{\sum_{n=p+1}^{E} \sigma_n^2}}{\sqrt{\sum_{n=1}^{p} \sigma_n^2}} \right| < \epsilon \right\} \tag{45}$$

Then the singular value decomposition (SVD) of the matrix $[\mathbf{Y}]$ is carried out as:

$$[\mathbf{Y}] = [\mathbf{U}] [\mathbf{\Sigma}] [\mathbf{V}]^H \tag{46}$$

where $[\mathbf{U}] \in \mathbb{C}^{(2S-L+1)\times(2S-L+1)}$ and $[\mathbf{V}] \in \mathbb{C}^{(L+1)\times(L+1)}$ are unitary matrices. $[\mathbf{\Sigma}] = \mathrm{diag}\{\sigma_1, \sigma_2, \dots, \sigma_M, \dots, \sigma_E; \sigma_1 \geq \sigma_2 \geq \dots \geq \sigma_E\}$ with $\{\sigma_i\}$ being the ordered singular

values of $[\mathbf{Y}]$, and $E = \min\{2S - L + 1, L + 1\}$. The lowest rank Hankel matrix $[\mathbf{Y}_P]$, which minimizes the LSE is defined as:

$$[\mathbf{Y}_P] = [\mathbf{U}] [\mathbf{\Sigma}_P] [\mathbf{V}]^H \tag{47}$$

Once the matrix $[\mathbf{Y}_P]$ has been calculated, the second step consists of using the MPM to estimate the parameters $\{z_n^*\}$ corresponding to the position of the new P array elements. For this purpose, the following generalized eigenvalue problem must be solved:

$$\left\{ \left([\mathbf{V}_{P,b}]^H [\mathbf{V}_{P,b}] \right)^{-1} \left([\mathbf{V}_{P,t}]^H [\mathbf{V}_{P,t}] \right) - \mathbf{z}^* \right\} \tag{48}$$

where $[\mathbf{V}_{P,b}] \in \mathbb{C}^{L \times P}$ (respectively $[\mathbf{V}_{P,t}] \in \mathbb{C}^{L \times P}$) is obtained after deleting the top row (respectively the bottom row) of $[\mathbf{V}_P] \in \mathbb{C}^{(L+1) \times P}$. The matrix $[\mathbf{V}_P]$ if formed by the first P singular vectors taken from the left side of $[\mathbf{V}]$ shown in (47).

Using Eq. (48) the parameters z_n^* were obtained, then it is possible to calculate the new position of the antenna elements and excitations as:

$$d_n^* = \frac{1}{jk\Delta} \log(\hat{z}_n^*); \quad j = \sqrt{-1} \tag{49}$$

$$I_n^* = \left(\left[\hat{\mathbf{Z}} \right]^H \left[\hat{\mathbf{Z}} \right] \right)^{-1} \left[\hat{\mathbf{Z}} \right] \overline{\mathrm{AF}}_{\mathrm{ref}}(u_s) \tag{50}$$

where

$$\hat{z}_n^* = \frac{z_n^*}{|z_n^*|} \tag{51}$$

$$\overline{\mathrm{AF}}_{\mathrm{ref}}(u_s) = (\mathrm{AF}_{\mathrm{ref}}(-S), \mathrm{AF}_{\mathrm{ref}}(-S+1), \ldots, \mathrm{AF}_{\mathrm{ref}}(S))^T \tag{52}$$

$$
\left[\hat{\mathbf{Z}} \right] = \begin{bmatrix}
(\hat{z}_1^*)^{-S} & (\hat{z}_2^*)^{-S} & \cdots & (\hat{z}_P^*)^{-S} \\
(\hat{z}_1^*)^{-S+1} & (\hat{z}_2^*)^{-S+1} & \cdots & (\hat{z}_P^*)^{-S+1} \\
\vdots & \vdots & \ddots & \vdots \\
(\hat{z}_1^*)^{S} & (\hat{z}_2^*)^{S} & \cdots & (\hat{z}_P^*)^{S}
\end{bmatrix}_{(2S+1)\times P}
\tag{53}
$$

Taking into account that this synthesis technique is based on Prony's method (Hua & Sarkar, 1990), the new position of the antenna elements d_n^* can be complex in those cases where $|Z_n^*| \neq 1$. However, since the calculation of the excitation currents shown in (50) is obtained using a least squares approximation, it is possible to discard the imaginary part of d_n^* without noticeably affecting the antenna array performance.

4.5   Chapter Summary

The mathematical modeling for the design of multiple-beam forming networks based on CORPS technology for scannable multi-beam antenna arrays has been presented in this chapter. The design of CORPS-BFN for multi-beam systems is introduced with three different approaches, where the evolutionary optimization is applied as a fundamental tool to obtain near-optimal solutions to the complex inputs to feed the network. Thus, the author presents the design of CORPS-BFN for linear and planar antenna array geometries and an additional approach for the design of a simplified feed network based on CORPS structures with the non-iterative matrix pencil method. The mathematical modeling introduced in this chapter is used in the next one, which presents the simulation and analysis of different case studies based on the previously introduced approaches.

5. Design of Beam-forming Networks for Multi-beam Antenna Arrays based on CORPS: Part II - Case Studies

5.1 Introduction

This chapter presents various case studies related to the design of CORPS beam-forming networks for antenna arrays. Each case study is related to a specific design approach presented in the previous chapter which are continued in this second part.

The cases studies are intended to show the possible benefits and performance of the network. Furthermore, each case study presents one or more original and specific configurations of CORPS. The range of options to propose CORPS network configurations are vast as discussed in Chapter 3, Section 3.3.1. Therefore, network configurations must be carefully proposed by the designer depending on several factors, such as the type of antenna array that feed, the number of beams to handle, and the target application.

On the other hand, it should be noted that all simulations in this chapter and in general the whole thesis were developed in the MATLAB simulation environment.

5.2 Design Approach of a CORPS-BFN for a Multi-beam Linear Antenna Array

5.2.1 Case study

To demonstrate the potential of CORPS technology applied to a beam forming network that feeds a set of antenna elements, in this work the next 2-beam design configuration is analyzed:

The configuration proposed shown in Figure 14 is a linear array system of 20 array antenna elements with 19 feeding ports (i.e. $M = 19$ and $N = 20$) implemented as a CORPS-BFN of one layer, with 10 complex inputs to control 11 antennas (beam #1) and 9 complex inputs to control 10 antennas (beam #2). In this manner, for this particular configuration an orthogonal signal could be conformed and controlled by the first 10 of the 20 feeding ports and the other 9 remaining to be used for another orthogonal signal, thus both signals can be scanned toward different or very close spatial locations.

The idea is to establish each group of inputs in a strategic way in order to have the capability to control electronically the corresponding beam pattern over a scanning range, considering the behavior of CORPS structures.
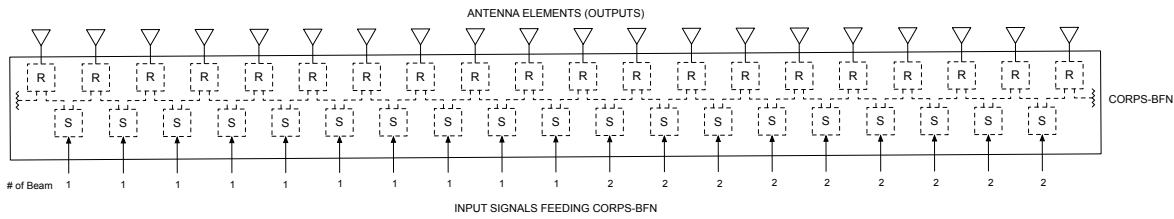
Figure 14. Proposed configuration of CORPS-BFN: ULA system of 19 feeding ports and 20 antenna elements considering 10 inputs × 11 outputs form beam #1 and 9 inputs × 10 outputs for beam #2.

The objective is to evaluate the behavior of the array factor generated by the configuration of CORPS-BFN for a steerable multi-beam linear array.

The evaluation of the array factor considers a steering range of 80 degrees, with an angular step of 10 degrees for a 20 elements antenna array and a uniform spacing between antenna elements of $\lambda/2$. In the same way, PSO was implemented for the optimization with the following parameters:

The optimization is executed using 200 individuals throughout 500 iterations to ensure a good sampling of the solution space, a global topology of PSO is used with a

time-varying inertial weight (ω) that decrease linearly from 0.9 to 0.4 throughout the iterations, the acceleration constants (c_1, c_2) are set to 2.0 and the maximum allowed velocity ($v_{d,max}$) is set as $\omega \cdot r$ where $r = (v_{d,max} - v_{d,min})$ (Arce $et\ al.$, 2009; Eberhart & Shi, 2001; Jin & Rahmat-Samii, 2007; Khodier & Christodoulou, 2005).

To perform a comparative analysis of the linear array system that considers CORPS-BFN as a feed network and the system without it, the following case study is proposed: in this study are analyzed 3 different cases, a uniform linear array (ULA) without optimization (i.e. the natural response of the array), a linear array considering the optimization of amplitude and phase without the use of CORPS-BFN, and finally a linear array fed by a CORPS-BFN with a proposed configuration (Figure 14).

This study provides information about the performance of the system in different configurations to conform a steerable radiation pattern. Thus, the study is based on the trade-off between side lobe level and directivity. Moreover, in the configuration that uses CORPS-BFN is expected an inherent simplification of the network in terms of the hardware used.

Note that to make a fair analysis in this case study, the behavior of one formed beam is studied and the number of control signals (inputs of the system) used to control the beam are the reference.

The obtained results from simulations are explained below.

5.2.2 Simulation results

Figures 15 and 16 show the performance in side lobe level and directivity respectively. In both figures different design cases are considered in which 10 control signals are taken for controlling just one beam through the scanning range. This scanning range is set

between $50° \leq \theta_0 \leq 130°$, with an angular step of $10°$.

In Figure 15 the isolation level from the main beam with respect to secondary lobes in different directions of interest are evaluated. The ULA conventional case is outweighed by the design case that optimizes both amplitude and phase perturbations with PSO but without CORPS-BFN. This optimized case reaches slightly higher values under -20dB in all the steering range. On the other hand, the behavior of CORPS-BFN configuration reaches the best performance with numerical values under -24dB when the direction of interest is near broadside region.
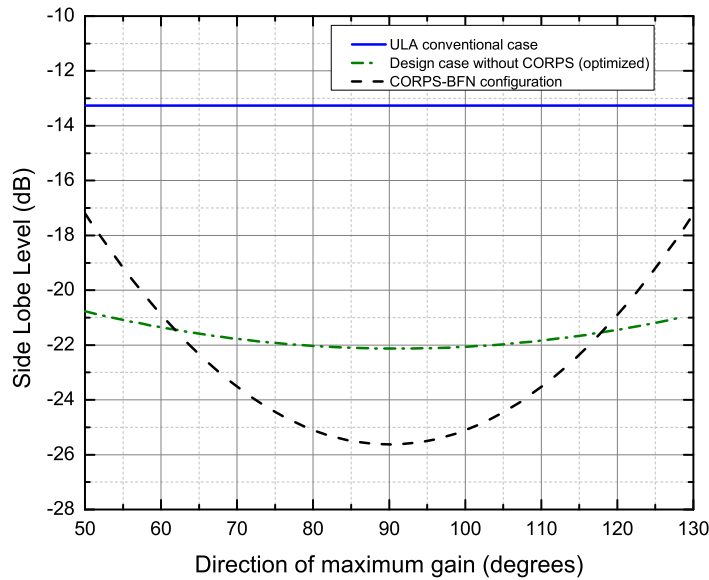
Figure 15. Side lobe level with respect to the steering direction of interest.

The directivity in different spatial directions of interest is evaluated in Figure 16. In this figure similar values of directivity between the optimized case without CORPS and the CORPS case with respect to the ULA conventional case are shown, with values between 9.5 to 10dB at 90 degrees for the three cases.

It is interesting to note that the values of SLL shown in Figure 15 achieving a better performance by the CORPS-BFN case and the directivity near the ULA case
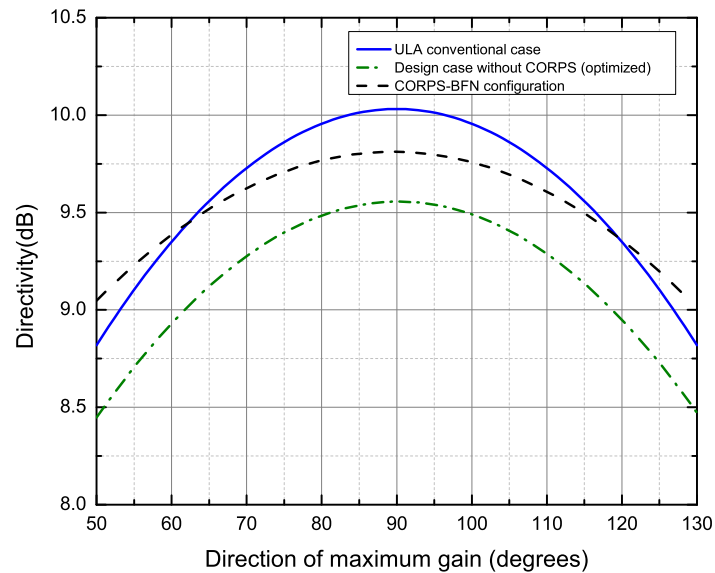
Figure 16. Directivity with respect to the steering direction of interest.

configuration reached by the same CORPS-BFN configuration in Figure 16, relies on the fact that CORPS-BFN allows to handle more antenna elements (in this case 11 antenna elements) with just 10 control inputs (i.e. a CORPS-BFN of one layer), showing that a network simplification can be made, reducing the number of control signals to handle more antenna elements to improve the performance.

The only disadvantage shown by the simulations is related to the visible window of approximately 70° which maintains the side lobe level under -20dB in this confined area (see Figure 15). Despite the above, CORPS-BFN has unique features that make it a good candidate for beam forming networks.

In Figure 17, it is shown an example of the radiation pattern of 2-beam system conformed by the configuration proposed optimized with PSO. This figure shown the CORPS-BFN capabilities to handle SLL and directivity to specific spatial locations. The orthogonal beams can scan the main beam towards highly nearby angles, with the advantage of not being a switched beam forming network (e.g. Butler matrix) and

control a fully adaptive radiation pattern.
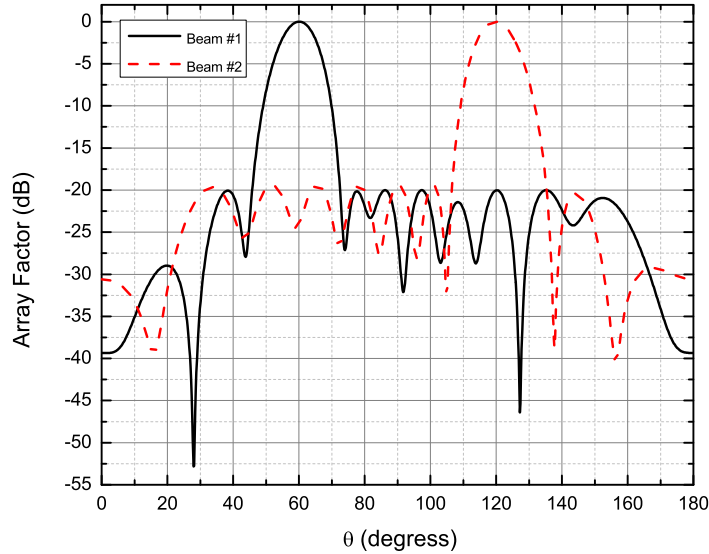
Figure 17. Array factor obtained by CORPS-BFN (the beam #1 is set to 60 degrees and beam #2 to 120 degrees).

The array factor behavior conformed by the CORPS system is showed in Figure 17, the direction of interest is set to 60° for beam #1 and 120° for beam #2. This particular configuration of CORPS only permits to control a subset of antenna elements of the array for each beam pattern. However, desired SLL could be remained in a wide scanning range with a good directivity response (see Figure 15 and Figure 16). The orthogonal beams generated and scanned are conformed with $N - 1$ complex inputs feeding the CORPS-BFN.

Finally, to complete the analysis, Figure 18 shows the specific values in amplitude and phase perturbations, related to the SLL and D obtained by computing the corresponding array factor generated by CORPS-BFN with the 2-beam design in Figure 17. This figure provides valuable information for possible implementation in hardware. The analysis demonstrates that the amplitude and phase excitations that feeds the CORPS-BFN optimized by PSO algorithm can achieve a good performance covering the most
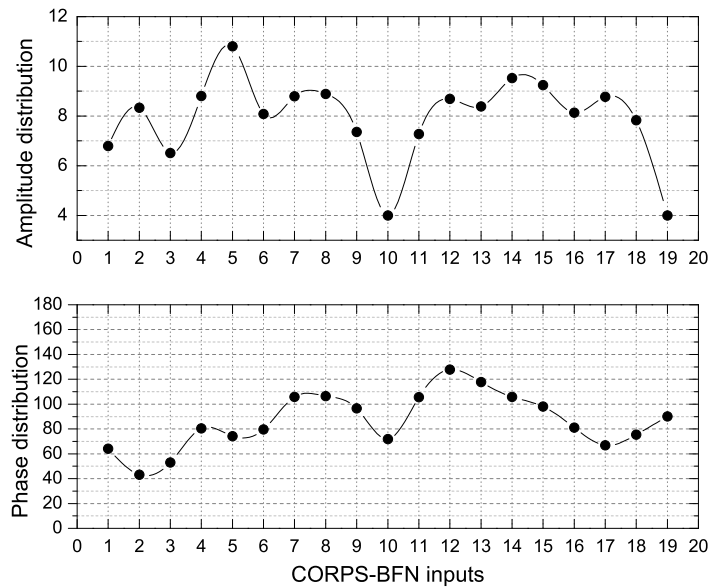
Figure 18. Amplitude and phase distributions at the input ports of CORPS-BFN for the example showed in Figure 17.

important trade-off between SLL and directivity, allowing this configuration to be a good alternative to be implemented in a multi-beam scenario.

5.2.3 Discussion on a CORPS-BFN for linear arrays

The design of a multi-beam BFN based on a configuration of CORPS for scannable antenna arrays using optimization has been introduced. Simulation results reveal that the design of multi-beam CORPS-BFN optimizing the complex inputs with PSO algorithm could cover the most important requirements to feed antenna arrays. The CORPS-BFN configuration studied and analyzed showed the advantages and drawbacks of adopting this technology. Highlighting the support to conform orthogonal multiple beams with the reduction of control signals (simplification of the BFN) to electronically scan the beam pattern over a wide range. Particularly, the CORPS-BFN configuration based in the control of a subset of antenna elements for each beam pattern demonstrated a

good performance complying the essential requirements in terms of SLL and directivity. Depending on the design requirements (scanning, directivity and the simplification of the network), a suitable configuration can be set. Future work will deal with different CORPS-BFN configurations (e.g. more layers) and designing CORPS-BFN for multi-beam planar (bidimensional) arrays searching to extend the advantages of the system.

5.3 Design Approach of a CORPS-BFN for a Multi-beam Planar Antenna Array

5.3.1 Case study

To analyze the performance of a multi-beam CORPS-BFN in a planar antenna array, it is proposed a configuration capable of controlling 9 orthogonal beams simultaneously. Furthermore, taking advantage of unique features of CORPS technology it is proposed a novel way to feed the network for the planar array. In this proposal the control of the 9 beams is realized by alternating input ports in subgroups where the input ports are reused by more than one signal or beam as illustrated in Figure 19.

The idea is to establish each group of inputs in a strategic way in order to have the capability to control electronically the corresponding beam pattern (over a scanning range) with a smaller number of complex inputs with respect to the number of radiators employed, considering the behavior of CORPS structures.

The CORPS feed network system was established defining the structure of CORPS-BFN system in 2 stages to feed the planar array(similarly to the methodology in Section 3.3.2). Each stage is composed for N CORPS-BFN blocks of one dimension. These blocks collectively integrate a complete CORPS-BFN system (2D CORPS-BFN) shown

in Figure 19.
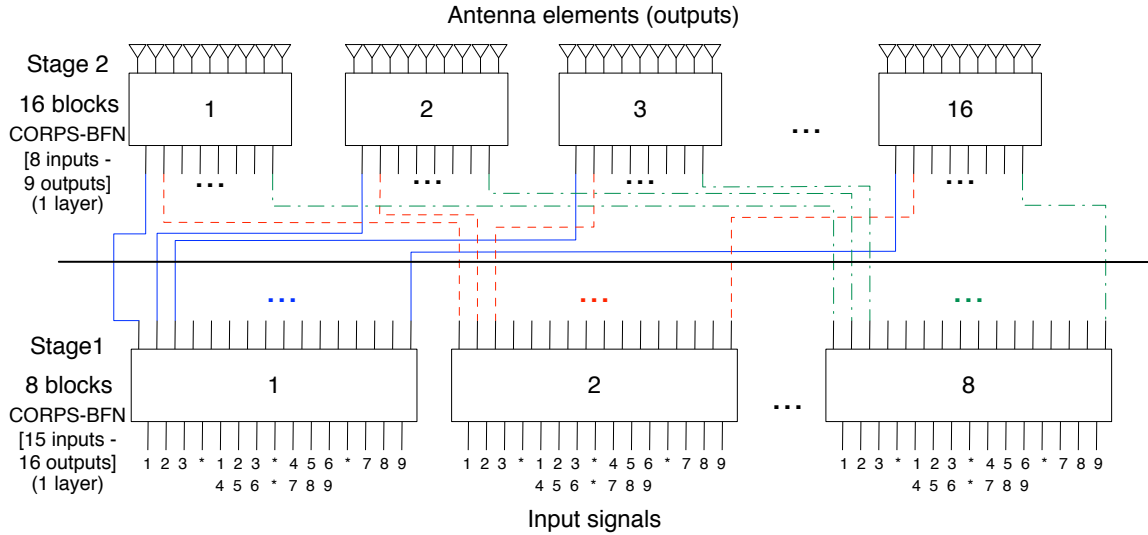
Figure 19. Network configuration of the CORPS-BFN system.

The first stage is formed by 8 CORPS-BFN blocks of one dimension with 15 input ports and 16 output ports. The index in each input port shown in Figure 19 indicates the number of beam or signal introduced that is related to a group of complex inputs for each beam, i.e. the index number 1 of each CORPS-BFN block belongs to the group of complex inputs for the beam #1 and so on for the 9 beams (the asterik denotes that the index input is not excited).

The second stage is formed by 16 CORPS-BFN blocks of one dimension with 8 input ports and 9 output ports. The 8 input ports of each of the 16 CORPS-BFN blocks in this stage are connected to the 16 output ports of each of the 8 CORPS-BFN blocks of the first stage. The stages are connected as follows: the 8 input ports of the first CORPS-BFN block in the second stage are connected to the first output of each of the 8 CORPS-BFN blocks of the first layer, the 8 input ports of the second CORPS-BFN block in the second stage are connected to the second output of each of

the 8 CORPS-BFN blocks of the first stage and so on for all CORPS-BFN blocks in the second stage.

Furthermore, as shown in Figure 19 the input index of each CORPS-BFN block of the second stage is determined by the index of the CORPS-BFN block of the first stage, e.g. the 2nd input port of the 1st CORPS-BFN block of the second stage is connected to the 1st output port of the 2nd CORPS-BFN block of the first stage.

In the CORPS-BFN system shown in Figure 19 there are a total of 144 outputs after the second stage feeding a planar array of 12×12 antenna elements as shown below in Figure 20.
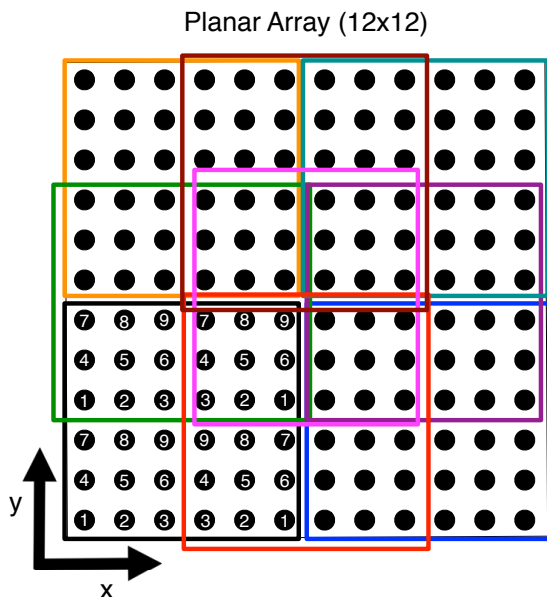
Figure 20. Distribution of the 9 beams within the planar array structure.

The planar array structure in Figure 20 is fed by the network described above. The complete multi-beam system is designed to generate 9 orthogonal beams simultaneously. This multi-beam system design is achieved through the reuse of input ports for more than one beam together with the natural overlap between adjacent beams in the CORPS

feed network, to finally obtain an efficient radiating aperture reuse.

In Figure 20 each beam is formed by a subset of 36 antenna elements (6×6 antenna subarray). The beam #1 is generated by the antenna elements in the bottom left of the array (black square), beam #2 is generated in the bottom center of the array (red square), beam #3 is generated in the bottom right of the array (blue square), beam #4 is generated in the center left of the array (green square), beam #5 is generated in the center of the array (pink square), beam #6 is generated in the center right of the array (purple square), beam #7 is generated in the top left of the array (orange square), beam #8 is generated in the top center of the array (brown square) and beam #9 is generated in the top right of the array (cyan square).

Finally, the same Figure 20 shows the detailed interconnection for beam #1 between the CORPS-BFN blocks of the second stage and the planar array structure. The first 3 rows and columns in the bottom left of the black square (3×3 antenna elements) are the outputs of the first CORPS-BFN block with indices from 1 to 9 (first group of outputs). The second group of outputs in the bottom right of the black square are the outputs of the second CORPS-BFN block. The third and fourth group of outputs in the top of the black square are the outputs of the third and fourth CORPS-BFN block respectively. As shown in Figure 20, the third and fourth group of outputs have the same interconnection than the first and second group of outputs. This interconnection is repeated for each of the 9 beams throughout the planar array structure.

The objective is to evaluate the behavior of the array factor generated by the complete CORPS-BFN system that includes a specific configuration for a steerable multi-beam planar array and demonstrate the possibilities of simplification and the performance advantages of using a CORPS-BFN on a planar array.

The method of GA was implemented to study the behavior of the array factor

(Che & Bian, 2008; Marcano & Duran, 2000; Soltankarimi *et al.*, 2004) generated by the configuration shown in Figure 19. The evaluation of the array factor generated in the azimuth plane in the cut of $\theta = 90°$ considers a steering range of $320°$ with an angular step of $40°$ for a planar array of $12×12$ antenna elements and a uniform spacing between antenna elements of 0.5λ. The parameters are set based on previous experience in solving antenna problems (Arce *et al.*, 2009; Reyna & Panduro, 2008). After a trial and error procedure for a parameter tuning, the parameters of the algorithm were set as follows: the GA algorithm is executed using 1000 individuals (population size) throughout 1000 iterations (the stopping criterion is based on the number of iterations) to ensure a good sampling of the solution space, with a crossover probability $P_c = 1.0$ and mutation probability $P_m = 0.1$. A selection scheme combining fitness ranking and roulette wheel selection was implemented (Goldberg, 1989; Eiben & Smith, 2003). The used genetic operators are standard: the well-known two point crossover (Goldberg, 1989; Eiben & Smith, 2003) along with a single mutation where a locus is randomly selected and the allele is replaced by a random number uniformly distributed in the feasible region of the search space.

5.3.2 Simulation results

Figure 21 shows an example of the array factor of the 9-beam system generated by the CORPS-BFN system previously presented in Section 5.3.1. The system is a planar array of $12×12$ (144 antenna elements) and 120 input ports with 16 complex inputs to control 36 antennas for each beam.

The optimized radiation pattern shows the CORPS-BFN capabilities to handle SLL and directivity in specific spatial locations for each of the 9 beams. Furthermore, the
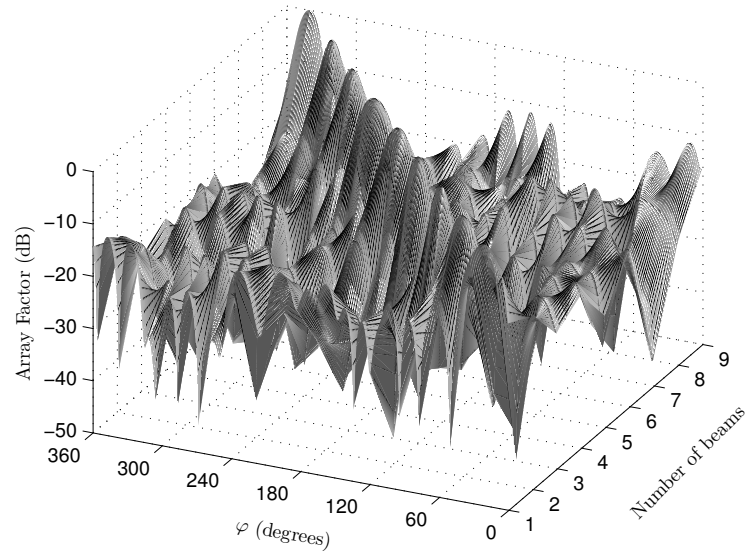
Figure 21. Array factor of the planar array generated by CORPS-BFN system with complex excitations optimized by GA in the cut of 90°.

coherent network can scan each main beam to any desired direction using just 16 input ports for 36 antenna elements. In this specific case the direction of maximum radiation is directed along the axis φ and set in $\varphi_0 = 20°$ for beam #1, $\varphi_0 = 60°$ for beam #2, $\varphi_0 = 100°$ for beam #3, $\varphi_0 = 140°$ for beam #4, $\varphi_0 = 180°$ for beam #5, $\varphi_0 = 220°$ for beam #6, $\varphi_0 = 260°$ for beam #7, $\varphi_0 = 300°$ for beam #8 and $\varphi_0 = 340°$ for beam #9.

Furthermore, in Figure 22, as a complement to Figure 21, shows the radiation intensity of the CORPS-BFN system. In this figure it is easy to observe the main beam steering of each of the 9 beams generated. The specific numerical values of side lobe level, directivity, and amplitude and phase distributions for the array factor illustrated in Figure 21 is shown in Table 1.

Table 1 shows the numerical values of side lobe level and directivity obtained by simulation, related to specific values in amplitude and phase perturbation distributions

Table 1. Numerical values of SLL and D with its amplitude and phase distributions for the array factor shown in Figure 21.

# of Beam	φ_0(deg)	SLL(dB)	D(dB)	Amplitude distribution	Phase distribution(deg)
1	20	-11.94	8.93	10.3970, 7.1140, 5.0772, 2.3355, 5.9640, 4.9668, 9.5763, 3.7475 8.3780, 2.9796, 7.9701, 12.5188, 1.2965, 7.8029, 5.6345, 4.6073	128.52, 96.03, 43.66, 88.50, 150.82, 58.60, 122.73, 103.16, 133.14, 108.33, 85.61, 88.84, 169.88, 110.13, 90.34, 122.43
2	60	-15.24	9.91	11.1752,1.3147,11.1378 9.9898,11.9785,12.8518, 7.9790, 4.4019, 9.2311, 12.6083,4.6889,13.0916, 3.4131, 13.5388, 6.3963, 10.2621	117.29, 120.53, 71.40, 136.71, 117.41, 99.98, 109.29, 159.27, 108.83, 105.53, 50.00, 54.30, 104.30, 90.13, 105.06, 104.02
3	100	-17.39	11.52	4.7913, 8.8830, 7.9199, 11.5519, 5.7256, 7.1472, 4.8219, 4.1242, 11.9429, 6.9350, 1.9021, 12.1611, 2.6526, 5.5082, 12.2492, 10.4667	84.23, 114.21, 36.61, 44.49, 61.07, 90.34, 113.40, 78.95, 57.26, 78.52, 55.17, 78.27, 95.82, 39.96, 107.12, 79.65
4	140	-17.91	11.31	11.1752,12.3125,8.2230, 12.0261, 7.9044, 7.2317, 7.2871, 7.9878, 10.5441, 5.8969,11.6612,13.5075, 7.0840, 7.9167, 4.9503, 10.2835	133.67, 66.28, 95.58, 114.76, 79.91, 50.69, 159.68, 89.20, 96.11, 124.97, 127.86, 86.33, 109.82, 102.99, 60.12, 143.35
5	180	-17.63	9.97	8.4864, 6.1150, 5.0772, 8.9706, 4.2146, 13.4937, 7.2871, 4.3038, 10.8085, 3.6832, 12.7302, 8.8640, 3.6862, 13.1437, 7.4750, 2.7377	56.20, 56.72, 49.90, 79.71, 69.81, 54.98, 59.80, 58.67, 58.76, 6.50, 29.78, 64.25, 10.12, 93.02, 19.71, 32.99
6	220	-15.55	9.25	8.4358, 8.7695, 9.2161, 10.9215,10.0031,12.1396, 1.9475, 9.8252, 4.6369, 10.8872,12.0958,11.0501, 12.1975,13.9435,1.1768, 7.5696	104.71, 89.34, 117.21, 102.87, 33.95, 80.82, 21.57, 87.47, 48.68, 78.52, 101.04, 94.33, 128.58,110.47, 172.19, 110.39
7	260	-14.02	10.46	9.9980, 8.9644, 8.9533, 4.3969, 5.4302, 11.3319, 1.4845, 5.0934, 7.85158, 12.4186,11.6293,13.5205, 6.6252, 7.0011, 5.6654, 1.1798	88.01, 124.36, 95.58, 163.43, 73.32, 44.27, 127.69, 89.20, 100.05, 40.12, 112.63, 41.28, 52.71, 50.78, 7.67, 32.99
8	300	-19.07	11.30	12.2955, 0.2421,11.3812, 7.5728, 5.7256, 10.6813, 9.5463, 2.7598, 10.1114, 4.8048, 7.9727, 4.8329, 9.5378, 5.9465, 13.7190, 4.5325	90.03, 114.21, 66.66, 153.94, 91.44, 91.89, 32.97, 96.85, 133.14, 175.77, 138.22, 125.64, 152.74, 36.72, 82.23, 27.27
9	340	-11.65	10.32	9.4791, 6.4995, 10.8822, 13.4864,1.9367,13.7053, 7.7487, 4.3038, 10.3445, 6.1279, 5.8839, 10.7617, 2.4835, 3.3369, 2.2222, 9.3555	118.06, 134.68, 109.97, 65.41, 172.05, 126.15, 78.32, 126.13, 113.53, 21.77, 114.16, 106.04, 1.19, 90.01, 141.35, 113.72
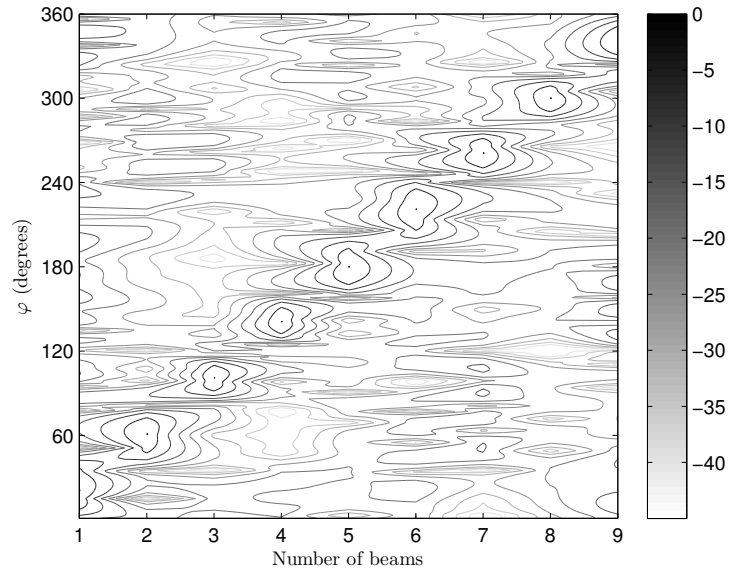
Figure 22. Radiation intensity for each of the 9 beams of the CORPS-BFN system.

for an example of the array factor generated by the 9-beam design of the CORPS-BFN system and illustrated in Figure 21. The table provides the evaluation of the array factor considering specific directions of maximum radiation previously defined. In this specific example, the optimization of array factor maintains a low SLL in almost all the scanning range. However, the relation between SLL and D degrade in two further angles from the broadside region $[20°, 340°]$. Furthermore, note that the orthogonal beams generated and scanned in this example are conformed with just 16 complex inputs and using an aperture of (6×6) 36 elements for each beam.

To perform a deeper analysis of the planar array that considers a CORPS-BFN system as a feed network, the trade-off between side lobe level and directivity on a wide visibility window over the azimuth plane φ is analyzed. Figures 23 and 24 show the performance in side lobe level and directivity for a scanning range between $20° \leq \varphi_0 \leq 340°$, with an angular step of $10°$.

The system using the CORPS-BFN under study shows a good performance in the
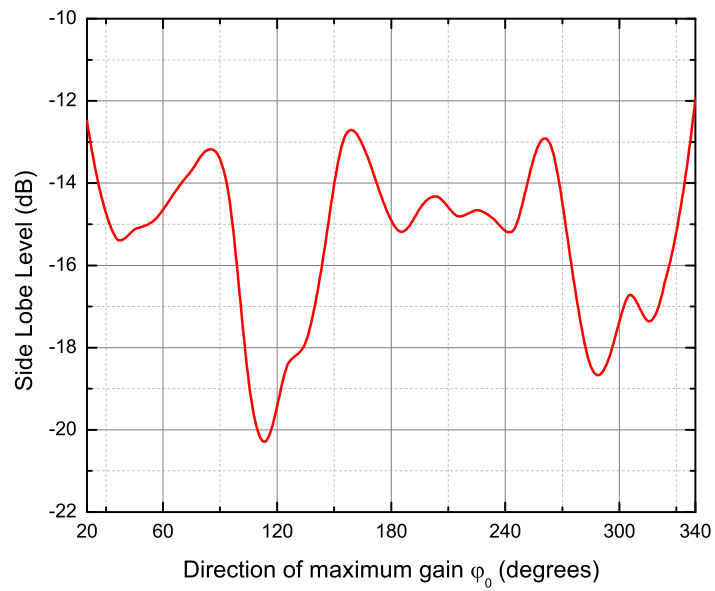
Figure 23. Behavior of the SLL with respect to the direction of interest.
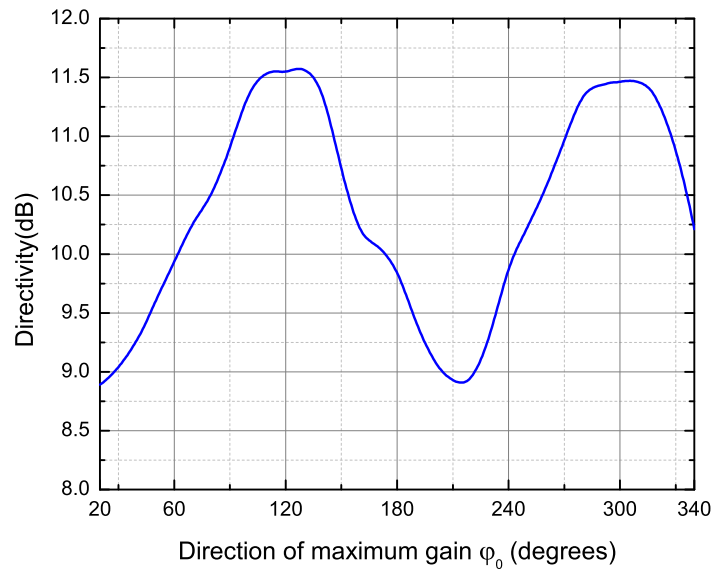
Figure 24. Behavior of the directivity with respect to the direction of interest.

scanning capability over a wide visibility window (320°). The complete system behavior generally remains constant throughout the steering range analyzed, i.e., almost constant values of SLL and D in a small window with numeric values approximately between 13dB to 16dB for the SLL and 9 to 10.5 for D. Except for two broad regions where a higher numerical values for the SLL and D are shown. The first region is located around 120° and the second around 300° approximately (see Figures 23 and 24).

The above performance is not achieved in linear arrays that use a CORPS-BFN where the scan angle range is small (about 80°). Also, at angles away from broadside region, these linear arrays show a decreasing behavior in terms of SLL and D, which worsens with the use of a greater number of layers (Panduro & del Rio Bocio, 2008; Panduro & del Rio-Bocio, 2009). Although in circular arrays using CORPS-BFN the overall performance (SLL and D) expected would be constant in all the scanning range, the network simplification is lower than the achieved in this approach for a planar array (Panduro & del Rio-Bocio, 2011).

5.3.3 Discussion on a CORPS-BFN for planar arrays

A specific case to generate nine scannable beams was presented, but it is possible to define different configurations choosing independently the number of antenna elements and the number of input ports (depending on the number of simultaneous orthogonal beams required).

In general, it is important to note the significative simplification of the complex inputs. Each of the 9 scannables beams is generated with $(N/2) - L$ complex inputs, i.e. the relationship between the complex inputs (M) and the number of antenna elements (N) for this particular configuration is less than $N/2$ for each beam ($N/2 - 2$

specifically for the proposed configuration). In addition, the technological advantages offered by CORPS to reuse antenna elements between adjacent beams (reducing the antenna array aperture) must be added to the simplification of the number of control inputs as discussed before. The above improvements offer a substantial simplification of the feed network.

In this way, the less limited scanning features in a planar array using CORPS as a feed network, make the network a better candidate for a greater number of applications that are based on the scanning capability. Moreover, in this type of scanning applications where the feed system (including all the associated electronic circuitry) is very complicated, the simplification of the feed network could be more significant for a planar (bidimensional) array.

Although only an example of CORPS-BFN for a planar array based on simulation is presented, depending on the design requirements and needs for a particular application a more convenient configuration can be easily established and implemented.

5.4   Design Approach in the Simplification of a CORPS-BFN using the Matrix Pencil Method

5.4.1   Case study

To demonstrate the compression capabilities of the matrix pencil method together with CORPS technology applied to a linear antenna array, two configurations of 2-beam design are proposed, as follows:

1. The first configuration (Figure 25) is a linear array system of 20 antenna elements with 19 feeding ports (i.e. $M = 19$ and $N = 20$) implemented as a CORPS-BFN

of one layer. In this case, the configuration use 10 complex inputs to control 11 antennas (beam #1) and 9 complex inputs to control 10 antennas (beam #2). In this type of configuration based in subgroups of input ports, an orthogonal beam could be conformed and controlled by the first 10 of the 20 feeding ports and the other subgroup of 9 could be used for another orthogonal beam.

2. The second configuration shown in Figure 26 considers a similar linear array system of 20 antenna elements with 19 feeding ports (CORPS-BFN of one layer). In this configuration the control of the 2 beams is realized by alternating input ports allowing that a group of 10 complex inputs could control the whole antenna array (20 antenna elements) for beam #1, and the 9 inputs remaining can control 18 of 20 antenna elements for beam #2.
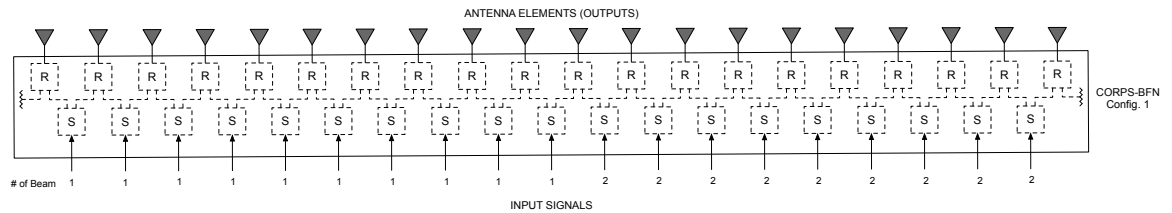
Figure 25. Configuration 1 of CORPS-BFN with 19 feeding ports and 20 antenna elements in a linear array considering 10 inputs × 11 outputs for beam #1 and 9 inputs × 10 outputs for beam #2.
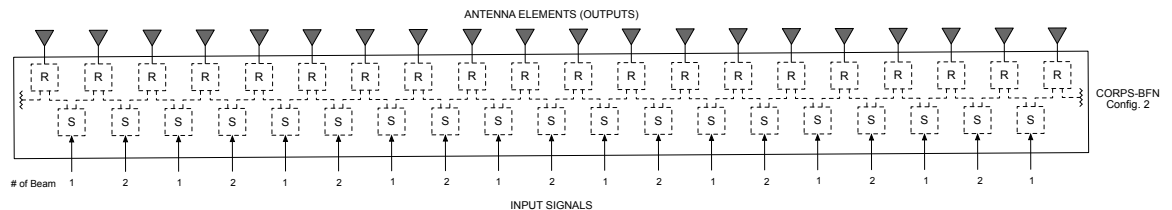
Figure 26. Configuration 2 of CORPS-BFN with 19 feeding ports and 20 antenna elements in a linear array considering 10 inputs × 20 outputs for beam #1 and 9 inputs × 18 outputs for beam #2.

The objective is to evaluate the behavior of the array factor generated by the two configurations of CORPS-BFN for steerable multi-beam linear arrays. The above for the purpose of analyze the possibilities of simplification and the performance advantages of using CORPS-BFN on a linear arrays. Furthermore, the results are compared with the same configurations of CORPS-BFN under study but adding the matrix pencil method to the antenna elements for a possible performance improvement.

The method of PSO was implemented to find a set of complex inputs to feed the configurations of CORPS-BFN shown in Figures 25 and 26 based on the same objective function as the one used in (37). This is in order to study the behavior of the array factor generated by both configurations (reference patterns). The evaluation of the array factor considers a steering range of $80°$, with an angular step of $10°$ for a linear array of 20 antenna elements with a initial uniform spacing of 0.5λ.

The parameters of PSO are set based on previous experience in solving antenna problems (Arce *et al.*, 2009, 2012b). After a trial and error procedure for a parameter tuning, the parameters of the algorithm were set as follows: the PSO algorithm is executed using 200 particles (population size) through 500 iterations to ensure a good sampling of the solution space, a global topology of PSO is used with time-varying inertial weight (ω) that decrease linearly from 0.9 to 0.4 throughout the iterations, the acceleration constants (c_1, c_2) are set to 2.0 and the maximum allowed velocity ($v_{d,max}$) is set as ωr where $r = (v_{d,max} - v_{d,min})$ in (35) (Arce *et al.*, 2009, 2012b; Eberhart & Shi, 2001; Jin & Rahmat-Samii, 2007; Khodier & Christodoulou, 2005).

In the case of the MPM, the error ξ of the reconstructed or approximated pattern generated is defined as:

$$\xi = \frac{\displaystyle\int_{-1}^{1} |\mathrm{AF_{ref}}(u) - \mathrm{AF_{MPM}}(u)|^2 \, du}{\displaystyle\int_{-1}^{1} |\mathrm{AF_{ref}}(u)|^2 \, du} \tag{54}$$

The metric in (54) assess the degree of optimality of the redesigned array defining the error over the reconstructed array factor $\mathrm{AF_{MPM}}$ with respect to the reference $\mathrm{AF_{ref}}$.

5.4.2   Simulation Results

To develop a comprehensive comparative analysis of the linear array system that just considers CORPS-BFN and the system with CORPS-BFN plus the matrix pencil method, first it is analyzed the array factor behavior in the two configurations of CORPS-BFN (Figures 25 and 26).

Figures 27 and 28 show an example of the radiation pattern of a 2-beam system generated by the configuration 1 of CORPS-BFN. This particular example shows the beam #1 (controlling 10 inputs for 11 outputs in Figure 27) and beam #2 (controlling 9 inputs for 10 outputs in Figure 28) of the configuration 1 (Figure 25). This configuration was previously optimized by PSO, showing the CORPS-BFN capabilities to handle SLL and for scanning the beam to a specific spatial location with certain directivity.

Furthermore, this one-dimensional array factor obtained in each figure define the reference for the compression process realized by the MPM. The array factor response of this additional method added to the configuration of CORPS-BFN (reconstructed pattern) is also shown in Figures 27 and 28 and is compared directly with the response of CORPS-BFN (reference pattern).

As can be seen in both figures, the CORPS-BFN plus the MPM almost exactly reproduce the desired pattern generated by the CORPS-BFN with $\xi = 0.041$ at $100°$

for beam #1 (Figure 27) and $\xi = 0.012$ at 80° for beam #2 (Figure 28) (for values of ξ in all the steering range, see Table 2). In the reduction process of the MPM the number of samples of the reference array factor (sampling points) is defined. From Nyquist sampling theorem at least $(2N - 1)$ samples are suitable.
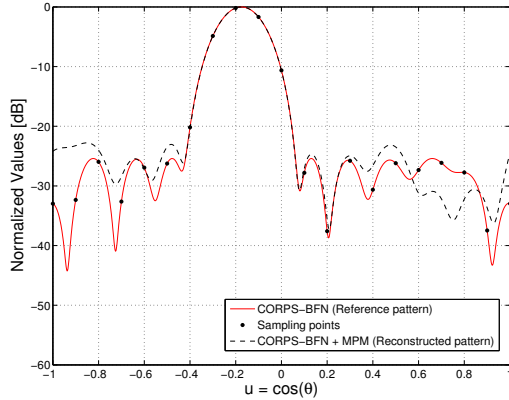
Figure 27. Comparison between the reference factor (CORPS-BFN) and the reconstructed factor (MPM+CORPS-BFN) obtained by the configuration 1 of the CORPS-BFN, showing an example of the beam #1 directed at 100°.
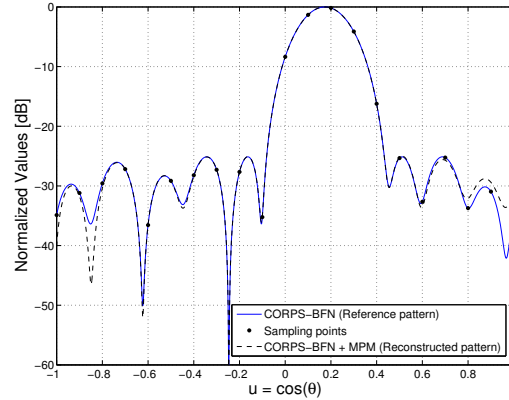
Figure 28. Comparison between the reference factor (CORPS-BFN) and the reconstructed factor (MPM+CORPS-BFN) obtained by the configuration 1 of the CORPS-BFN, showing an example of the beam #2 directed at 80°.

Similarly, Figure 29 shows the same comparison made in Figures 27 and 28 using the configuration 2 of the CORPS-BFN for the beam #1. In this specific example the beam is controlled by 10 inputs ports for 20 outputs (alternating inputs ports see Figure 26). Despite the whole array is controlled by the half of input ports, the array factor formed by CORPS-BFN (reference pattern) in this example shows high levels of side lobe level ($SLL \approx -5dB$) and the approximation pattern generated by the CORPS-BFN plus the MPM in this configuration presents a value of $\xi = 0.137$ at 70° for beam #1, showing side lobes almost similar to the main lobe. This could be a disadvantage in some steering directions, however a complete analysis of configuration

Table 2. Error ξ for the antenna steering in each evaluated configuration.

| Angle(Deg) | Error ξ | | | |
| | Configuration 1 | | Configuration 2 | |
	Beam #1	Beam #2	Beam #1	Beam #2
50	0.4177	0.3612	-	-
60	0.4741	0.4863	-	-
70	0.0299	0.0770	0.1372	0.0973
80	0.0136	0.0124	0.4412	0.4116
90	0.0224	0.0039	0.1332	0.0302
100	0.0411	0.0177	0.4771	0.4097
110	0.0698	0.0524	0.1015	0.0973
120	0.5200	0.5067	-	-
130	0.5294	0.2546	-	-

2 is presented in Table 2.

Additionally, Figure 30 represents the singular value spectrum of the CORPS-BFN pattern samples for the configurations of CORPS-BFN shown in Figures 27 and 28. The singular values in the two cases decay rapidly with just few small singular values that can be discarded. Based on the above, the reference pattern can be reconstructed with an smaller aperture (see Figures 31 and 32).

Furthermore, in Table 3 the values of ϵ for each angle of steering for the configuration 1 are shown (ϵ depends on how accurately the reconstructed pattern approximates the reference radiation pattern).

The comparison between the example of CORPS-BFN (reference pattern) and the CORPS-BFN plus the MPM (reconstructed pattern) in terms of amplitude and element location (λ) is shown in Figures 31 and 32.

As can be seen in both figures, the MPM redistributes the magnitude of the current and the location of each antenna element, taking advantage of the new non-uniformity of the linear array which results in a reduction of the antenna elements. Given that the
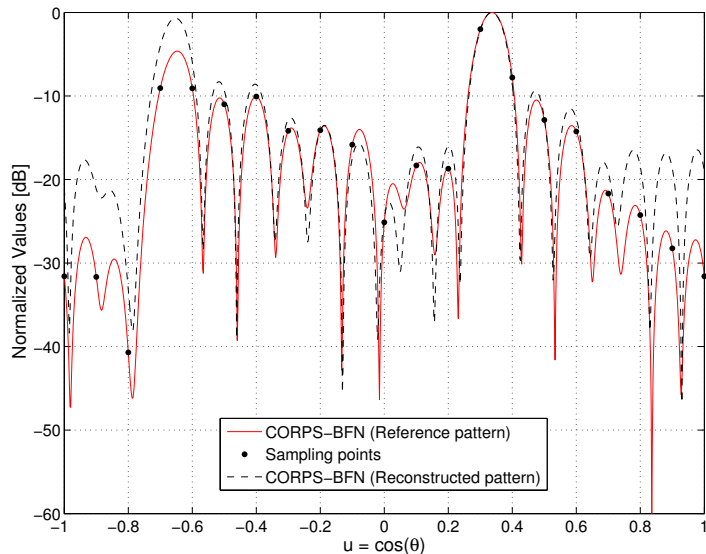
Figure 29. Comparison between the reference factor (CORPS-BFN) and the reconstructed factor (MPM+CORPS-BFN) obtained by the configuration 2 of the CORPS-BFN, showing an example of the beam #1 directed at 70°.
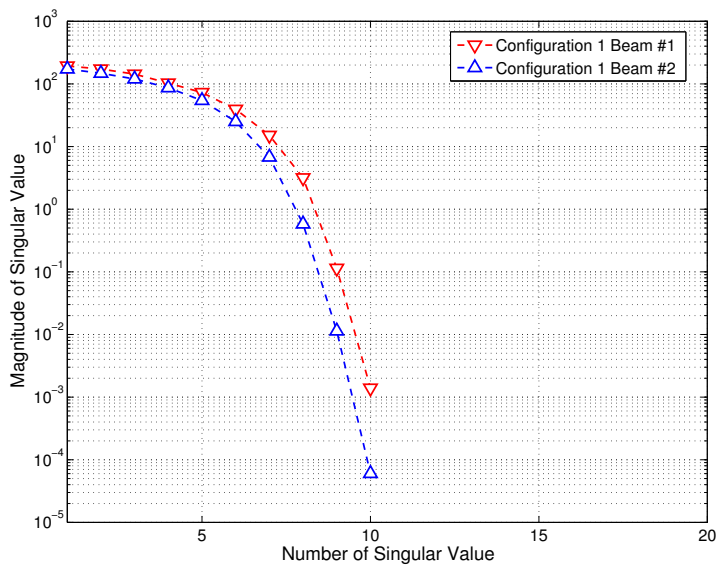
Figure 30. Singular value spectrum of the CORPS-BFN configuration 1, for the example based in Figures 27 and 28.

Table 3. Value of ϵ for each angle of steering.

Angle(Deg)	Value of ϵ	
	Beam #1	Beam #2
50	10^{-8}	10^{-7}
60	10^{-8}	10^{-8}
70	10^{-7}	10^{-8}
80	10^{-5}	10^{-8}
90	10^{-5}	10^{-5}
100	10^{-7}	10^{-5}
110	10^{-7}	10^{-8}
120	10^{-8}	10^{-9}
130	10^{-8}	10^{-9}

compression for beam #1 (Figure 31) are 2 antenna elements and for beam #2 is just 1 antenna element (Figure 32), in a CORPS-BFN of one layer (this case study where $M = N - 1$) implies that also reduces 2 input ports for beam #1 (i.e. the 10 inputs × 11 outputs for beam #1 are reduced to 8 inputs × 9 outputs to generate the beam) and 1 input port for beam #2 (i.e. the 9 inputs × 10 outputs for beam #2 are reduced to 8 inputs × 9 outputs to generate the beam).

If the entire system is considered (i.e. beam #1 and #2) there is a significant reduction of the whole CORPS-BFN system. Considering the complete configuration 1, the 19 feeding ports and 20 antenna elements are reduced to 16 feeding ports and 17 antenna elements considering 8 inputs for 9 outputs for beam #1 and 8 inputs for 9 outputs for beam #2, with a good approximation of the reference patterns.

To develop a more complete analysis of the two configurations under study, then it is analyzed the trade-off between the steering angle (visible window) and the error of the reconstructed pattern (54) generated by the MPM.

Figures 33 and 34 show the error of the beam #1 (line with squares) and beam #2 (line with diamonds) for each configuration of CORPS-BFN (Figures 25 and 26)
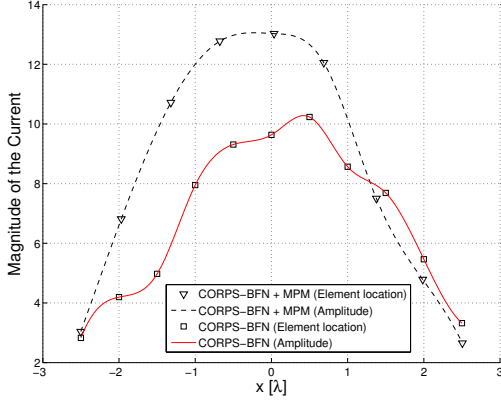
Figure 31. Amplitude distribution and antenna element location for the reference factor (CORPS-BFN) and the reconstructed factor (MPM + CORPS-BFN) for the beam #1 shown in Figure 27.
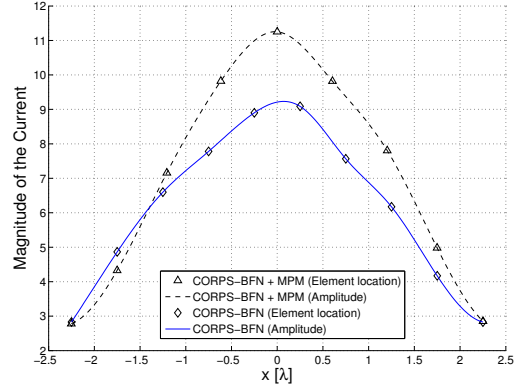
Figure 32. Amplitude distribution and antenna element location for the reference factor (CORPS-BFN) and the reconstructed factor (MPM + CORPS-BFN) for the beam #2 shown in Figure 28.

analyzed. The scanning range is considered between $50° \leq \theta_0 \leq 130°$ and $70° \leq \theta_0 \leq 110°$ with an angular step of $10°$ for the configuration 1 (Figure 33) and 2 (Figure 34) of CORPS-BFN, respectively.

The configuration 1 of CORPS-BFN (Figure 33) shows a good performance in the scanning capability for the 2 beams analyzed with high values of error only at the ends of the steering range over the visibility window ($50°$-$130°$). For the case of the configuration 2 of CORPS-BFN (Figure 34) both beams present a similar behavior with a small difference between them. In the configuration there are two regions whith high numerical values of error ξ (values between 0.4 to 0.5), the first region has its peak at $80°$ and the second at $100°$ in a smaller visible window ($70°$-$110°$).

5.4.3 Discussion on the simplification of a CORPS-BFN using the Matrix Pencil Method

Although, two specific cases to generate two scannable beams were presented, it is
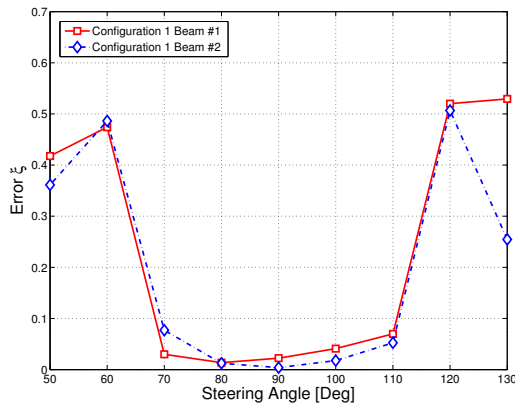
Figure 33. Behavior of the error ξ with respect to the direction of maximum gain for the configuration 1 of CORPS-BFN.
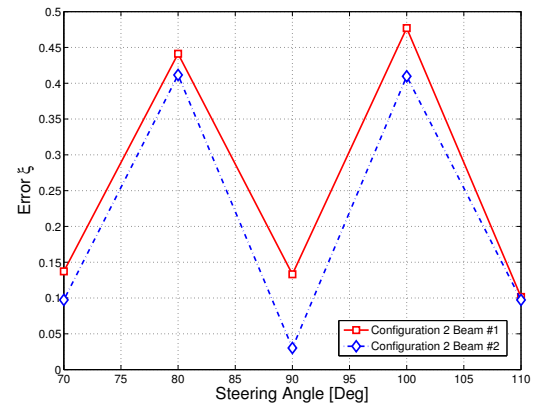
Figure 34. Behavior of the error ξ with respect to the direction of maximum gain for the configuration 2 of CORPS-BFN.

possible to define different configurations varying the number of antenna elements and the number of input ports depending on the number of independent beams required.

In general, it is important to note the significative simplification offered by the combination of CORPS-BFN with the compressive method of MPM. On one side the intrinsic technological advantages offered by CORPS-BFN itself (e.g. reuse antenna elements between adjacent beams, reduction of control signals, etc.). On the other hand the MPM improvements added to the CORPS-BFN technology and demostrated in this approach based on the reduction of the aperture, taking advantage of the relocation of antenna elements (using the non-uniformity of the antenna array) and the redistribution of complex excitations. Thus, a reduction in the antenna array by the MPM results in a reduction in the CORPS-BFN (including all the associated circuitry, i.e. inputs ports, power combiners and splitters). The above improvements offer a substantial simplification of the feed network for linear arrays.

In this way, the lower complexity of an entire antenna system (i.e. the antenna array and the beam-forming network subsystem) obtained by the CORPS-BFN plus

the matrix pencil method, make the system a good candidate for a great number of applications where the weight, size, and cost are important (e.g. satellite applications). Although our examples of CORPS-BFN plus the MPM for linear arrays are based on simulations, depending on the design requirements and possible application, more suitable configurations can be set and then be implemented.

5.5   Chapter Summary

Different study cases for each design approach based on CORPS were presented in this chapter. The first design approach for a multi-beam linear array presents a study case in which a comparison between three configurations of interest is made. One of them deals with a 2-beam design configuration of CORPS-BFN. Instead, the design approach for a multi-beam planar antenna array proposed and analyzed a study case based on a 9-beam design configuration of CORPS-BFN with aperture reuse and with an innovative way to feed it. Finally, the last design approach is focused on symplifying a CORPS network in which two 2-beam design configurations of CORPS-BFN for steerable linear array are proposed. In this study case the additional method of the matrix pencil method is applied to the antenna array with the objective of simplifying the antenna system.

6. CORPS-BFN on Cellular Mobile Communication Systems

6.1   Introduction

With the evolution of cellular mobile communication technologies, the demand for higher data rate services and the steadily growing user market on the limited available electromagnetic spectrum, motivate service providers to seek ways to improve communication system capacity and reliability.

Next-generation mobile technologies have proposed different multi-antenna techniques such as the spatial multiplexing[24] and transmitter-side beamforming (classical beamforming) to solve in some part the aforementioned problematic (Döttling *et al.*, 2009).

In the case of beamforming in multiple transmit antennas, the antenna array may typically contain a switched-beam based on beam-forming networks (BFNs) or on fully adaptive configurations using phased arrays. Thus, switched-beam arrays create fixed, simultaneous and multiple beams. On the other hand, adaptive arrays conform and direct the beam pattern by utilizing signal-processing algorithms (Mailloux, 1994).

Recently a technology called Coherently Radiating Periodic Structures (CORPS) has been introduced as an alternative beam-forming network that can be used to feed a phased array (Betancourt & del Rio Bocio, 2007). In this way, an antenna array system based on CORPS technology may have adaptive features together with the capability of generating multiple orthogonal beams.

In a mobile cellular communication scenario, a CORPS system could discern nearby

---

[24]Term often also referred to as MIMO (Multiple-Input Multiple-Output).

users without affecting adjacent beams and to service users separated by a small angular position. With these properties, the networks based in CORPS that form an entire antenna system are an attractive option to increase SINR[25] by providing directed beams to multiple users simultaneously, increasing the user capacity of a cell and the spectral reuse.

In this chapter, the use of CORPS technology is introduced in the application of mobile communications. Two configurations of a beam-forming network feeding an antenna array using CORPS in a base station (BS) are presented.

CORPS-BFN is applied in a multi-user mobile scenario, where the particle swarm optimization (PSO) algorithm optimizes the required amplitude and phase excitations that should be introduced to the network. This design strategy deals with an important trade-off in mobile communications such as side lobe level (SLL) and signal-to-interference ratio (SIR) improvement capability (Durrani & Bialkowski, 2002a) in an appropriate coverage range. The main contribution of this chapter is to propose the CORPS-BFN technology as an efficient and innovative beam-forming network alternative in cellular systems. In this way, this novel network introduces interesting features that can be applied in a multi-beam mobile communication scenario.

6.2 System Modeling

To model a complete antenna system that considers the design of a beam-forming network for a steerable multi-beam antenna array using coherently radiating periodic structures in a mobile communication system is indispensable to use the CORPS-BFN model introduced in Section 3.3.1. Then assuming a linear array for the design, it is

---

[25]Signal-to-interference-plus-noise power ratio.

essential to use the design approach for a linear array previously presented in Chapter 4, in Section 4.2. The steps for this process are clearly explained and can be implemented using (29) to (34).

Subsequently, it is necessary to use an optimization process to obtain the complex excitations to feed the beam-forming network. In this case the PSO algorithm is used again and can be implemented as in Section 4.2.2. However, the objective function must be redefined to consider metrics of interest in cellular systems, as described below:

Let $m = \varphi_1, \varphi_2, \ldots, \varphi_M$ be the set of M angles where the beam pattern with its main lobe in the direction of the desired user θ_1 is steered. Let $\mathbf{G}_{\mathrm{avg}} = G_{\mathrm{avg}}(\varphi_1, \mathbf{a}, \mathbf{p})$, $G_{\mathrm{avg}}(\varphi_2, \mathbf{a}, \mathbf{p}), \ldots, G_{\mathrm{avg}}(\varphi_M, \mathbf{a}, \mathbf{p})$ be the set whose elements are the SIR improvement coefficients for the m elements. In this way, based on these definitions and considering the objective function in (37), the objective function can be rewritten as:

$$
\begin{aligned}
minimize \quad & (|\mathrm{AF}(\theta_{\mathrm{SLL}}, \mathbf{a}, \mathbf{p})|/\max|\mathrm{AF}(\theta, \mathbf{a}, \mathbf{p})|) + \max(\mathbf{G}_{\mathrm{avg}}) \\
subject\ to \quad & A_i \in \mathbb{A} \ \text{and} \ \xi_i \in \mathbb{P}, \quad \forall i = 1, 2, \ldots, N - L
\end{aligned}
\tag{55}
$$

where $\mathbb{A} = [4, 12]$ and $\mathbb{P} = [0, 180]$ are the amplitude and phase domains, respectively. The goal is to minimize the weighted sum that involves both objectives (SLL and SIR improvement capability respectively), which are uniformly weighted in the cost function.

Finally, it is necessary to develop the signal model employed to evaluate the performance of the system. This model is presented in the following subsection.

6.2.1   Signal Model

In order to evaluate the performance of the proposed CORPS-BFN, a signal model is required to estimate SIR improvement capability. This interference rejection capability

is function of the number of antenna elements (including the total aperture) and the direction of signal arrival of a chosen user and the interferers (Durrani & Bialkowski, 2002a). Using this figure of merit is sought to provide maximum interference reduction.

The signal model for investigating the SIR improvement capability of uniform linear arrays fed by a CORPS-BFN is developed by making several assumptions in order to reduce the problem of array performance evaluation to a more manageable complexity.

These assumptions are mentioned below. It is considered that the dimensions of the antenna arrays are small compared to the distances from mobile signal sources[26]. Also, it is assumed that the angular distribution of users is uniform[27].

In addition, it is defined that line-of-sight paths exist between the system and all users, excluding effects such as mutual coupling, scattering and multipath fading from consideration. These effects aforementioned can be integrated with the results of this work, but that is beyond the scope of it.

The system at the base station receives signals from K narrow-band mobile users, which are randomly distributed in the xy-plane (azimuthal direction) in the far-field of the array. The location of each user is through its angle of arrival (AoA) contained in θ. Using vector notation, the received signal can be expressed as (Durrani & Bialkowski, 2002a):

$$\mathbf{x}(t) = \sum_{k=1}^{K} \boldsymbol{a}(\theta_k)s_k(t) + \mathbf{n}(t) = \mathbf{A}(\theta)\mathbf{s}(t) + \mathbf{n}(t) \tag{56}$$

where $\mathbf{x}(t)$ is an $N \times 1$ vector of measured voltages, $\mathbf{s}(t)$ is a $K \times 1$ signal vector, $\mathbf{n}(t)$ is an $N \times 1$ noise vector, and $\mathbf{A}(\theta) = [\boldsymbol{a}(\theta_1), \boldsymbol{a}(\theta_2), \ldots, \boldsymbol{a}(\theta_k)]$ is an $N \times k$ matrix whose columns are steering vectors of the sources. The $N \times 1$ steering vector $\boldsymbol{a}(\theta_k)$ models

---

[26]i.e., to deal with far-field effects and to assume that the incoming waveforms are planes waves.

[27]In other words, the system has users uniformly distributed along the circumference of a circle with the base station at its center.

the spatial response of the array due to an incident plane wave from θ direction and $s_k(t)$ is the signal transmitted by the kth source as received by the reference antenna.

Let $s_1(t)$ be the desired signal source arriving from direction θ_1 and consider the rest of the signals $s_k(t)$, $k = 2, 3, \ldots, K$, as interferences arriving form their respective directions. The array output is given by (Durrani & Bialkowski, 2002b, 2004):

$$y(t) = \mathbf{w}^H \mathbf{x}(t) \tag{57}$$

where $\mathbf{w}$ is the weight vector that is applied to the antenna array to produce a beam pattern with its main lobe in the direction of the desired user. Assuming that maximum signal-to-noise ratio beamforming is performed, $\mathbf{w}$ is given by:

$$\mathbf{w} = \frac{1}{N} \boldsymbol{a}(\theta_1) \tag{58}$$

Thus the array becomes the phased array as the magnitudes of the weight vector are constant and only the phases are varying. Substituting (58) and (56) into the array output (57) and simplifying, we get:

$$y(t) = s_1(t) + \frac{1}{N} \sum_{k=2}^{K} s_k(t) \boldsymbol{a}^H(\theta_1) \boldsymbol{a}(\theta_k) + \frac{1}{N} \boldsymbol{a}^H(\theta_1) \mathbf{n}(t) \tag{59}$$

The mean output power is:

$$P(t) = E\left[y(t) y^*(t)\right] = E\left[|s_1(t)|^2\right]$$
$$+ \sum_{k=2}^{K} \frac{1}{N^2} \left|\boldsymbol{a}^H(\theta_1) \boldsymbol{a}(\theta_k)\right|^2 \cdot E\left[|s_k(t)|^2\right] + E\left[\frac{1}{N} |\boldsymbol{a}_H(\theta_1) \mathbf{n}(t)|^2\right] \tag{60}$$
$$P(t) = E\left[|s_1(t)|^2\right] + \sum_{k=2}^{K} \alpha_k(\theta_1, \theta_k) E\left[|s_k(t)|^2\right] + \frac{\sigma^2}{N}$$

The first term on the right side of (60) is the desired signal power, whereas the second and third terms represent interference and noise power, respectively.

The coefficient given by:

$$\alpha_k(\theta_1, \theta_k) = \left(\frac{1}{N^2}\right) \left|\boldsymbol{a}^H(\theta_1)\boldsymbol{a}(\theta_k)\right|^2 \tag{61}$$

in (60) is a measure of how much undesired power is picked up from an interferer.

Assuming the interferers are uniformly distributed in the range $[0, \pi]$, the mean value of $\alpha_k(\theta_1, \theta_k)$ is expressed as:

$$G_{\text{avg}}(\theta_1) = E\left[\alpha_k(\theta_1, \theta_k)\right] = \frac{1}{\pi}\int_0^\pi \alpha_k(\theta_1, \theta_k)\, d\theta_k \tag{62}$$

where $G_{\text{avg}}(\theta_1)$ is the spatial interference suppression coefficient[28](Song & Kwon (1999); Durrani & Bialkowski (2004)). The coefficient $\alpha_k(\theta_1, \theta_k)$, after some manipulations and substituting the values from (31), (55), and (61) is given as:

$$
\begin{aligned}
\alpha_k(\theta_1, \theta_k, \mathbf{a}, \mathbf{p}) &= \left(\frac{1}{N^2}\right) \left|\boldsymbol{a}^H(\theta_1, \mathbf{a}, \mathbf{p})\boldsymbol{a}(\theta_k, \mathbf{a}, \mathbf{p})\right|^2 \\
&= \frac{1}{N^2}\left|\sum_{n=1}^N I_n e^{jkd_n(cos\theta_k - cos\theta_1)}\right|
\end{aligned}
\tag{63}
$$

Using (60), the instantaneous SIR at the array output (SIR$_\text{o}$) can be written as:

$$\text{SIR}_\text{o} = \frac{E\left[|s_1(t)^2|\right]}{\displaystyle\sum_{k=2}^K \alpha_k(\theta_1, \theta_k) E\left[|s_k(t)|^2\right]} \tag{64}$$

Hence, the mean SIR at the array output (SIR$_\text{o}$) can be written in terms of input SIR (SIR$_\text{in}$) as follows:

---

[28]This coefficient is directly related to the SIR improvement capability for the linear array.

$$\text{SIR}_\text{o} = \frac{\text{SIR}_\text{in}}{G_\text{avg}(\theta_1)} \tag{65}$$

The average improvement in SIR (Δ) at the array output is then given as:

$$\Delta = 10 \log_{10} \left(\frac{1}{G_\text{avg}(\theta_1)} \right) = -10 \log_{10} \left(G_\text{avg}(\theta_1) \right) \tag{66}$$

The output signal-to-interference-plus-noise power ratio in a cellular system is a function of the SIR at the array output (SIR_o) and can be written as (Song & Kwon, 1999):

$$\text{SINR}_\text{o}(\theta_1) = \frac{P_s}{I_o + N_o} = \frac{\text{SIR}_\text{o}(\theta_1) \cdot \text{SNR}_\text{o}}{\text{SIR}_\text{o}(\theta_1) + \text{SNR}_\text{o}} \tag{67}$$

where

$$\text{SNR}_\text{o} = N \cdot \text{SNR}_\text{in} \tag{68}$$

P_s is the output power of the desired user signal, I_o the total output power of the other user signals, N_o the noise output power, SNR_in the input signal-to-noise power ratio and SNR_o the output signal-to-noise power ratio.

In a Rayleigh fading environment, the bit error rate (BER) of a cellular system can be written as:

$$P_b = \frac{1}{\pi} \int_0^\pi \frac{1}{2} \left[1 - \sqrt{\frac{\gamma_b(\theta_1)}{1 + \gamma_b(\theta_1)}} \right] d\theta_1 \tag{69}$$

where

$$\gamma_b(\theta_1) = \frac{\text{SINR}_\text{o}(\theta_1)}{2} \tag{70}$$

The simulation scenario and results obtained are described below.

6.3 Simulation Setup and Results

6.3.1 Simulation case study

In this section, the potential of CORPS technology applied to a beam-forming network that feeds a set of antenna elements in a base station as part of a cellular system is demonstrated. For this purpose, two configurations of 2-beam design are proposed which are the same as presented in Section 5.4 and illustrated in Figures 25 and 26.

The objective is to evaluate the behavior of the array factor generated by the configurations 1 and 2 of CORPS-BFN for a steerable multi-beam linear arrays analyzing metrics of interest in cellular systems.

The evaluation of the array factor considers a steering range of 80º, with an angular step of 10º for a 20 elements antenna array and a uniform spacing between antenna elements of $\lambda/2$.

Furthermore, the system must meet important requirements in a cellular system such as the maximum interference reduction and SLL in an adequate steering range. Therefore, the PSO algorithm was implemented for the optimization of complex inputs in the CORPS configurations (Figures 25 and 26) using the objective function previously presented in (55) and the same parameters as in Section 5.4.

The obtained results from simulations are explained below.

6.3.2 Simulation results

With the objective to perform a comparative analysis of the antenna system that considers a CORPS-BFN and the typical way to feed the array (i.e., direct feeding to the antenna elements) in cellular systems. It is proposed the next study case: the case of a

uniform linear array (ULA) without optimization (conventional case), i.e. the natural response of the array, in the same way it is studied the behavior of the array factor for linear array considering the optimization of amplitude and phase without the use of CORPS-BFN. And finally, the case that considers a linear array with a CORPS-BFN with two proposed configurations (Figures 25 and 26).

This study provides information about the trade-off between performance of the system with different configurations to conform a steerable radiation pattern in terms of SLL and the SIR improvement capability.

And moreover, in the cases dealing with CORPS-BFN the simplification of the network is observed, in terms of the components used for the BFN. To make a fair analysis in this case study, the behavior of one conformed beam is studied and the number of control signals (inputs of the system) used to control the beam was the reference.

Figures 35 and 36 show the performance in side lobe level and signal-to-interference ratio (SIR) improvement capability, considering in both different design configuration cases and taking 10 control signals into account for controlling just one beam through the scanning range between, with an angular step of 10°.

In Figure 35 the isolation level with respect to main beam to secondary lobes in different directions of interest are evaluated. The ULA conventional case is outweighed by the design case that optimizes both amplitude and phase perturbations by PSO without CORPS-BFN reaching slightly higher values under -20dB in all the steering range. On other hand, the behavior of CORPS-BFN configuration 2 in terms in SLL is just appropriate at the broadside region decreasing its performance outside 90 degrees with valid values in a smaller steering range (70° to 110°). Finally, the performance of the CORPS-BFN configuration 1 reaches numerical values under -24dB when the

direction of interest is near of broadside region.
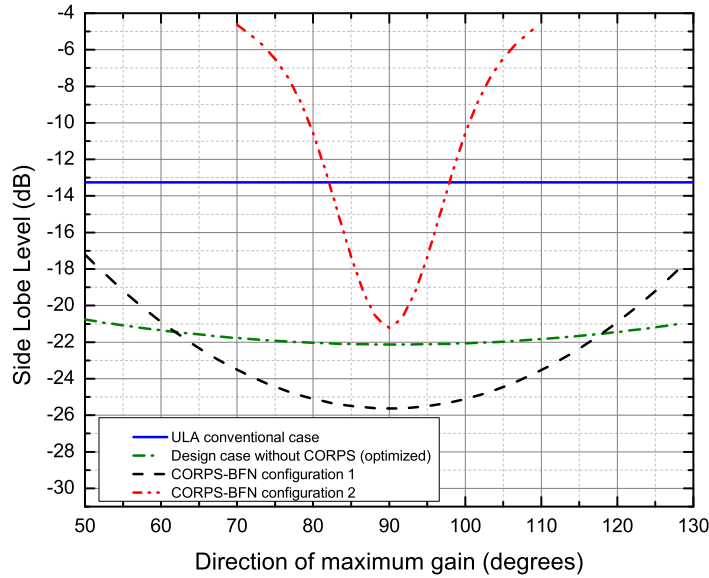
Figure 35. Side lobe level with respect to the steering direction of interest.

The SIR improvement $G_{\mathrm{avg}}(\theta_1)$ for all the cases in different spatial directions of interest is illustrated in Figure 36, showing similar values in SIR improvement capability between the optimized case without CORPS-BFN and CORPS-BFN configuration 1 with respect to ULA conventional case, with values approximately between 11.5 and 12 dB at 90 degrees for these three cases. High SIR improvement capability is obtained by CORPS configuration 2 with numerical values between 12.8 to 14.6 dB. The results in Figure 36, show that SIR improvement is maximum over a certain range of θ_1, centered at $\theta_1 = 90°$ (broadside). The discrimination against interferers (in terms of SIR) is best in the broadside direction of the array and deteriorates in its end-fire directions and similar or better values in the SIR improvement is dependent on the CORPS-BFN configuration chosen.

It is interesting to note that the values of SLL shown in Figure 35 achieving a better performance by CORPS-BFN configuration 1 and the SIR improvement capability near
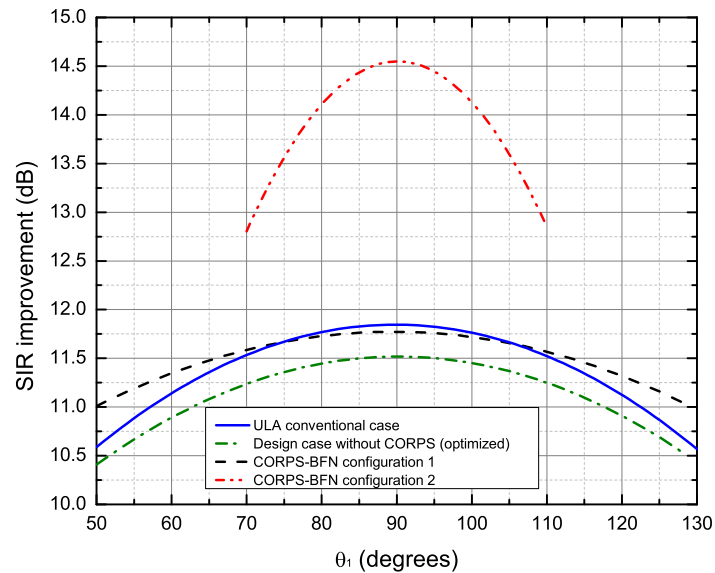
Figure 36. SIR improvement $G_{\mathrm{avg}}(\theta_1)$ variation with respect to θ_1.

to ULA case configuration reached by the same CORPS-BFN configuration in Figure 36, relies in that CORPS-BFN allows to handle more antenna elements (in this case 11 antenna elements) with just 10 control signals (i.e. CORPS-BFN of one layer), showing that a network simplification can be made, reducing the number of control signals to handle more antenna elements to improve the performance.

In the same way, it is important to highlight that CORPS-BFN configuration 2 in both figures is controlling electronically all the antenna array with just 10 feeding input ports, this configuration can obtain the highest SIR improvement capability over all the design configurations and a good performance in SLL with the same aperture in all designs when the direction of interest is near 90 degrees.

The only disadvantage shown by the simulations is related to the visibility window of approximately 70° and 10° for CORPS-BFN configurations 1 and 2 respectively, which maintain the isolation level of under -20dB in this confined area (see Figure 35) but for CORPS-BFN configuration 2 is compensated with its SIR improvement capability (see

Figure 36). Despite the above, CORPS-BFN has unique features that make it a good candidate for cellular applications.

The mean of SIR improvement $G_{\text{avg}}(\theta_1)$ in (dB) over θ_1 (an average of $G_{\text{avg}}(\theta_1)$ over the assumed range θ_1), the average SINR_{o} and BER for all the design cases under study are shown in Tables 4-6, considering 10 control signals ($M = 10$).

The average SIR improvement $G_{\text{avg}}(\theta_1)$, the output SINR and resulting BER for all the simulated cases were calculated using the expressions given previously. It is assumed a SIR_{in} of 7.2125 dB and SNR_{in} of 10 dB in accordance with Song & Kwon (1999). The simulation results are generated assuming uniformly located users in the range $[0, \pi]$. For each user, the SIR improvement, the SINR_{o} and resulting BER were calculated.

The values reveal that for the same number of control signals the ULA case, the design case optimized and the CORPS-BFN configuration 1 have nearly the same mean of G_{avg}, SINR_{o} and BER over θ_1. However, CORPS-BFN configuration 2 reveals slightly better values of these metrics as expected.

Figures 37 and 38 shown examples of the radiation pattern of 2-beam system conformed by the configuration 1 and 2 respectively, optimized with PSO, showing the CORPS-BFN capabilities to handle SLL and scan the beam to specific spatial locations. The completely orthogonal beams can scan the main beam towards a different

Table 4. Average SIR improvement $G_{\text{avg}}(\theta_1)$ over θ_1 for ULA, design case optimized and CORPS-BFN configurations.

Average SIR improvement $G_{\text{avg}}(\theta_1)$ over θ_1 for $M = 10$			
ULA	Design case optimized	CORPS-BFN configuration 1	CORPS-BFN configuration 2
11.4136	11.0604	11.4466	13.6869

Table 5. Average $SINR_o$ over θ_1 for ULA, design case optimized and CORPS-BFN configurations.

Average $SINR_o$ over θ_1 for $M = 10$			
ULA	Design case optimized	CORPS-BFN configuration 1	CORPS-BFN configuration 2
16.1731	16.0296	16.2621	17.3890

Table 6. Average BER over θ_1 for ULA, design case optimized and CORPS-BFN configurations.

Average BER over θ_1 for $M = 10$			
ULA	Design case optimized	CORPS-BFN configuration 1	CORPS-BFN configuration 2
0.0117	0.0120	0.0114	0.0089

or very close direction of interest, with the advantage of not being a switched beam-forming network (e.g. Butler matrix) and control a fully adaptive radiation pattern.

The array factor behavior conformed by the CORPS-BFN configuration 1 is showed in Figure 37, the direction of interest is set in 60° for beam #1 and 120° for beam #2. This particular configuration of CORPS only permits to control a subset of antenna elements of the array for each beam pattern. However, desired SLL could be remained in a wide scanning range with a good SIR improvement response (see Figures 35 and 36). The orthogonal beams generated and scanned are conformed with $N-1$ complex inputs feeding the CORPS-BFN.

In the same way, an example of the array factor of 2-beam design conformed by CORPS-BFN configuration 2 is shown in Figure 38. Despite the low performance in SLL away from broadside region (see Figure 35), high SIR improvement capability can be achieved near broadside region (see Figure 36). This configuration of CORPS-BFN permits to control more antenna elements with respect to the configuration 1 due its alternated feeding ports with the same number of control signals.
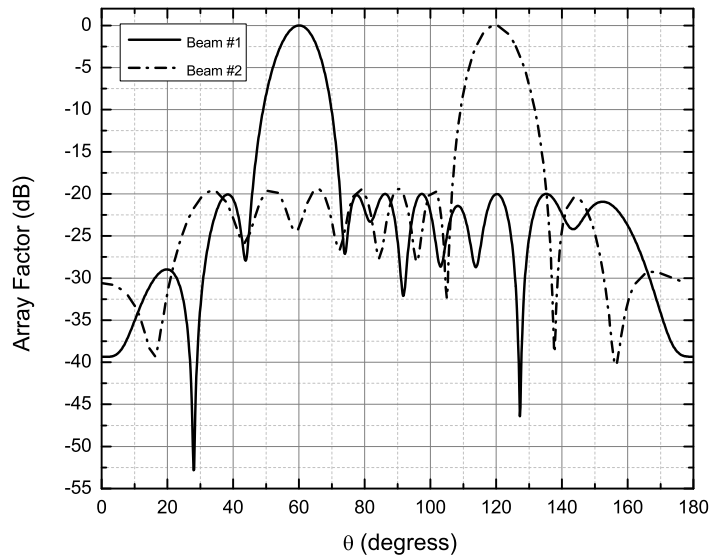
Figure 37. Array factor obtained by CORPS-BFN configuration 1 (the beam #1 is set in 60º and beam #2 in 120º.)
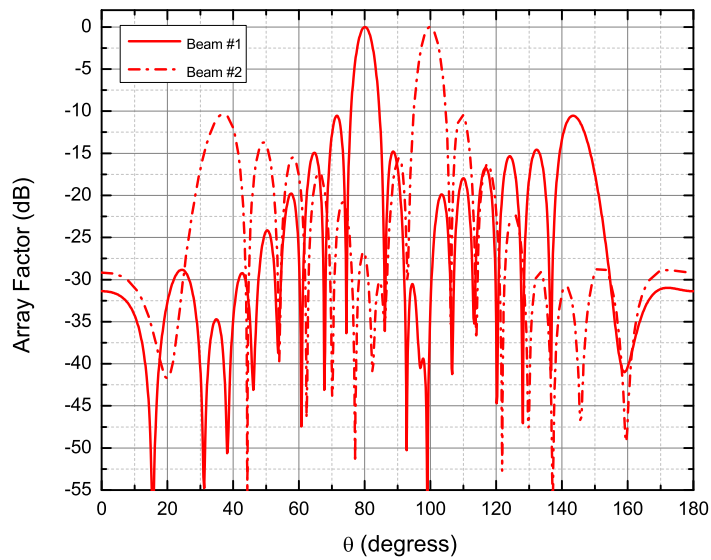
Figure 38. Array factor obtained by CORPS-BFN configuration 2 (the beam #1 is set in 60º and beam #2 in 120º.)
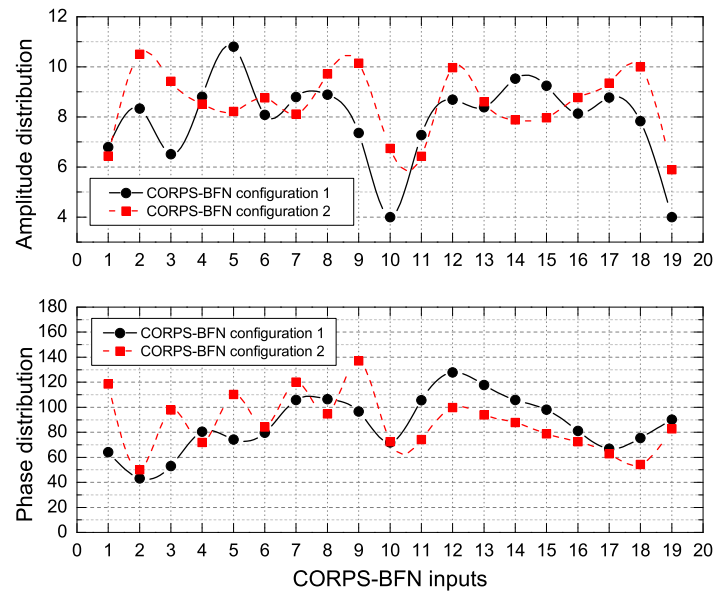
Figure 39. Amplitude and phase distribution at the input ports of CORPS-BFN configurations for the example shown in Figures 37 and 38.)

Finally to complete the analysis of the study, Figure 39 shows the specific values in amplitude and phase perturbations for the array factor generated by CORPS-BFN configurations 1 and 2 (Figures 37 and 38). These figures provide valuable information for possible implementation in hardware. The simulation analysis demonstrates that the amplitude and phase excitations that feed the CORPS-BFN optimized by PSO algorithm can achieve a good performance covering a trade-off between SLL and SIR improvement capability, allowing that the CORPS-BFN configurations become a good alternative to be implemented in cellular mobile communications.

6.3.3 Discussion on CORPS networks on cellular systems

The design of a multi-beam BFN based in a configuration of CORPS for scannable antenna arrays using optimization on mobile communication system has been introduced. Simulation results reveal that the design of multi-beam CORPS-BFN optimizing the complex inputs with PSO algorithm could attend multiple users covering the most

important requirements on this study and improving results over conventional way to feed antenna arrays and with more attractive features than existing BFNs. The CORPS-BFN configuration studied and analyzed showed the advantages and drawbacks of adopting this technology on a base station. Highlighting the support to conform orthogonal multiple beams to provide service with the reduction of control signals (simplification of the BFN) to electronically scan the beam pattern over a coverage area. Particularly, CORPS-BFN configurations based on the control of a subset of antenna elements for each beam pattern (configuration 1) and the configuration based in alternated feeding ports (configuration 2), demonstrated the best performance fulfilling essential requirements on cellular mobile communications in terms of SLL and SIR improvement capability, and improving results over the optimized design case and ULA conventional case. Moreover, this good performance is reflected in important metrics such as the output SINR and BER.

6.4 Chapter Summary

In this final chapter, the CORPS beam-forming networks on cellular mobile communication systems were introduced. Presenting metrics of interest in cellular systems that were translated to the objective function to optimize with the PSO algorithm. In addition, a complete signal model to estimate SIR improvement capability is presented. In this model several assumptions were made to reduce the complexity of this model.

Furthermore, two 2-beam design configurations of CORPS-BFN for multi-beam linear array on a cellular scenario were proposed and analyzed. Simulation results showed the benefits of beam-forming networks based on CORPS for a cellular scenario based on the array factor response. Moreover, results for the average SIR improvement, SINR and BER were discussed.

7. Conclusions and Future Research

This chapter concludes the research work and summarize the main contributions of this dissertation and also identifies future research lines related to the work done.

The research in this work has been focused mainly on different design approaches for beam-forming networks based on coherently radiating periodic structures including its introduction on cellular mobile communication systems. These CORPS beam forming networks are an emerging technology solution for systems requiring dynamic and reconfigurable multi-beam environments.

For this reason, the work was directed towards the study of the behavior of different design configurations of CORPS-BFN including the analysis of the network in different array geometries, contrasting the results with usual ways of feeding antenna arrays. Furthermore, these design configurations of CORPS-BFN allowed the introduction of evolutionary optimization approaches to BFN design as a supplement for the antenna pattern synthesis, achieving specific design goals on the beam shaping. In addition, advanced compression techniques employed in antenna synthesis were used for the simplification of the beam-forming network with interesting results. Finally, previous research allowed to introduce the CORPS beam-forming network in cellular mobile communication systems, analyzing metrics of interest. The research conducted and based on the above topics allowed to have a series of contributions to the state of art reflected in several publications. The main contributions of this work are presented in detail in the next section.

7.1 Contribution

At the beginning of this research, the problem of defining a beam-forming network and optimization algorithms based on a hypothesis defined a series of simulations and analysis with the following results:

- A performance evaluation in a first scenario related to uniform linear arrays in which it was used optimization algorithms (GA and PSO), showed that there was no improvement in performance in terms of better solutions but there was a better performance of PSO algorithm in computation time (Arce *et al.*, 2011).

- In a second scenario in which it was used linear arrays fed by a CORPS-BFN with a trade-off between side lobe level and directivity, it was chosen to use interchangeably either evolutionary algorithms (GA or PSO) in terms of performance. Furthermore, this study defined the CORPS-BFN as the network of choice for further investigations due to its performance in terms of beam scanning and its multi-beam properties (see Chapter 3), defining the direction of this work.

Therefore, the most important contributions of this work are related to the design of beam-forming networks based on coherently radiating periodic structures. So, the research work was divided into four different design approaches involving a CORPS network. In the first approach concerning to the design of a CORPS-BFN for a multi-beam linear antenna array, it can be highlighted the following (Arce *et al.*, 2012a; Arce-Casas *et al.*, 2011):

- The optimized CORPS beam-forming network for uniform linear arrays (ULA) proved to be an efficient and innovative alternative feed network and candidate for use in various applications, including cellular systems.

- Analysis of CORPS-BFN in linear arrays demonstrated attractive features in the design of feed networks such as the generation of multiple beams towards different targets or directions of interest, scanning of the main beams and especially the simplification of the network in terms of the control inputs required to generate and steer the beams. This study was conducted with an untreated evolutionary optimization approach in these structures, complementing previous work done by Betancourt & del Río (2006); Panduro (2007); Panduro & del Rio Bocio (2008).

- Furthermore, the simulation of CORPS-BFN for linear arrays was compared with usual feeding configurations for antenna arrays demonstrating advantages and compromises between the objectives treated (side lobe level and directivity).

The second approach in this work deals with the design of a CORPS-BFN for a planar antenna array, the most notable contributions in this study are enunciated below (Arce *et al.*, 2012c):

- The study of optimized CORPS-BFN was extended toward planar antenna arrays, in this case the network was capable of generating and scanning multiple orthogonal beams in a shared aperture.

- A significant reduction in the complexity of the network was demonstrated improving configurations proposed in the literature in different geometries (Panduro & del Rio Bocio, 2008; Panduro & del Rio-Bocio, 2009, 2011). This was achieved through a proposed network design and the reuse of the input ports reducing the antenna aperture.

The third approach addressed in this work is about the simplification of a beamforming network based on CORPS using an analytical compression technique called

matrix pencil method. The main findings of this study are described below (Arce *et al.*, 2012d):

- The non-iterative compression technique matrix pencil method used in the synthesis of antennas was introduced into a complete antenna system that uses a CORPS-BFN. The MPM method demonstrated its potential and limitations in linear arrays fed by a CORPS-BFN and in possible applications involving multiple independent beams and steering capabilities.

- The integration of the technique MPM and CORPS technology in an antenna system reduced the complete system including the antenna array (reducing the number of antenna elements) and the beam-forming subsystem (consequently reducing the number of control inputs) resulting in a significant simplification of the feed network.

The final approach is related to the introduction of the CORPS-BFN in the application of cellular mobile communication systems. The most important aspects of this approach are shown below (Arce *et al.*, 2012b; Arce-Casas *et al.*, 2011):

- The CORPS beam-forming networks were introduced and applied for the first time in cellular mobile communication systems offering good performances reflected in metrics of interest such as the average SIR improvement, SINR and BER.

- The CORPS-BFN compared against other conventional feeding cases in a linear array as a part of a base station, demonstrated its advantages and limitations, emphasizing the generation of multiple orthogonal beams and reduction in the number of control signals to control them but with the inconvenience of a small visible window in some network configurations.

7.2 Future Research

The objective of this section is to emphasize the lines of research to follow started in this work and to show aspects of this work that can be improved. In this manner, it is derived the following future research:

- With the purpose of improving the performance of CORPS beam-forming networks, future work may be related to the analysis of these networks in different antenna array geometries not yet studied (e.g., concentric rings arrays).

- The performance demonstrated by the CORPS-BFN in the current literature, make it suitable for use in various applications. Therefore, future research lines could be related to introducing and analyzing these networks in different applications such as radar and satellite systems.

- Aditionally, future work may be related to the simplification and efficiency of the CORPS networks through the design of new configurations.

- The results presented in this work are about different network configurations addressed in diverse approaches, with simulations based on the response of the antenna system as a function of their array factor. Therefore, future work could be related to a more realistic scenario through the use of electromagnetic simulators and/or the construction of prototypes.

References

Allen, B. & Ghavami, M. (2005). *Adaptive Array Systems: Fundamentals and Applications*. First Ed. Chichester, England, Wiley.

Arce, A., Covarrubias, D., & Panduro, M. (2009). Performance evaluation of population based optimizers for the synthesis of linear antenna arrays. In *Proceedings of the 6th IASTED International Conference on Antennas, Radar, and Wave Propagation (ARP)*, 103–108.

Arce, A., Covarrubias, D., & Panduro, M. (2011). Performance evaluation of stochastic algorithms for linear antenna arrays synthesis under constrained conditions. *Journal of Selected Areas in Telecommunications*, *2*(5), 41–47.

Arce, A., Covarrubias, D., Panduro, M., & Garza, L. (2012a). Design of beam-forming networks for multibeam antenna arrays using coherently radiating periodic structures. *Journal of Applied Research and Technology*, *10*(1), 48–56.

Arce, A., Covarrubias, D. H., & Panduro, M. A. (2012b). Design of a multiple-beam forming network using CORPS optimized for cellular systems. *International Journal of Electronics and Communications (AEU)*, *66*(5), 349 – 356.

Arce, A., Covarrubias, D. H., Panduro, M. A., & Garza, L. A. (2012c). A new multiple-beam forming network design approach for a planar antenna array using CORPS. *Journal of Electromagnetic Waves and Applications*, *26*(2-3), 294–306.

Arce, A., Yepes, L. F., Covarrubias, D. H., & Panduro, M. A. (2012d). A new approach in the simplification of a multiple-beam forming network based on CORPS using compressive arrays. *International Journal of Antennas and Propagation*, *2012*, 1–8.

Arce-Casas, A., Covarrubias-Rosales, D., & Panduro-Mendoza, M. (2011). Design of multibeam CORPS-BFN for cellular mobile communications systems. In *Proceedings of the 5th European Conference on Antennas and Propagation (EUCAP)*, 1272 –1276.

Balanis, C. (1992). Antenna theory: a review. *Proceedings of the IEEE*, *80*(1), 7–23.

Balanis, C. A. (1997). *Antenna theory : analysis and design*. Second Ed. New York, NY, John Wiley & Sons.

Betancourt, D. & del Río, C. (2006). Designing feeding networks with CORPS: coherently radiating periodic structures. *Microwave and Optical Technology Letters*, *48*(8), 1599–1602.

Betancourt, D. & del Rio, C. (2009). PSP planar lens: A CORPS BFN to improve radiation features of arrays. In *3rd European Conference on Antennas and Propagation (EuCAP)*, 1312–1315.

Betancourt, D. & del Rio Bocio, C. (2007). A novel methodology to feed phased array antennas. *IEEE Transactions on Antennas and Propagation*, *55*(9), 2489–2494.

Betancourt, D. & Rio, C. D. (2011). *The Coherently Radiating Periodic Structures: And their applications in Beam Forming Networks for Multiple-Beam Systems*. Saarbrucken, Germany, LAP LAMBERT Academic Publishing.

Blass, J. (1960). Multidirectional antenna - a new approach to stacked beams. In *IRE International Convention Record*, 8, 48–50.

Butler, J. & Lowe, R. (1961). Beam-forming matrix simplifies design of electronically scanned antennas. *Electronic Design*, *9*, 170–173.

Chang, C.-C., Lee, R.-H., & Shih, T.-Y. (2010). Design of a beam switching/steering Butler matrix for phased array system. *IEEE Transactions on Antennas and Propagation*, *58*(2), 367–374.

Che, X.-Q. & Bian, L. (2008). Low-side-lobe pattern synthesis of array antennas by genetic algorithm. In *4th International Conference on Wireless Communications, Networking and Mobile Computing (WiCOM)*, 1–4.

Corona, A. & Lancaster, M. (2003). A high-temperature superconducting Butler matrix. *IEEE Transactions on Applied Superconductivity*, *13*(4), 3867–3872.

Döttling, M., Mohr, W., & Osseiran, A. (2009). *Radio Technologies and Concepts for IMT-Advanced*. First Ed. Chichester, England, Wiley.

Durrani, S. & Bialkowski, M. (2002a). Interference rejection capabilities of different types of array antennas in cellular systems. *Electronics Letters*, *38*(13), 617 –619.

Durrani, S. & Bialkowski, M. (2004). Effect of mutual coupling on the interference rejection capabilities of linear and circular arrays in cdma systems. *IEEE Transactions on Antennas and Propagation*, *52*(4), 1130 – 1134.

Durrani, S. & Bialkowski, M. E. (2002b). An investigation into the interference rejection capability of a linear array in a wireless communications system. *Microwave and Optical Technology Letters*, *35*(6), 445–449.

Eberhart, R. C. & Shi, Y. (2001). Particle swarm optimization: developments, applications and resources. In *Proceedings of the 2001 Congress on Evolutionary Computation*, 1, 81–86.

Eiben, A. E. & Smith, J. E. (2003). *Introduction to evolutionary computing*. First Ed. New York, NY, Springer.

Engelbrecht, A. P. (2005). *Fundamentals of Computational Swarm Intelligence*. First Ed. Chichester, England, John Wiley & Sons.

Ferrando, N. & Fonseca, N. (2011). Investigations on the efficiency of array fed coherently radiating periodic structure beam forming networks. *IEEE Transactions on Antennas and Propagation*, *59*(2), 493–502.

Fonseca, N. (2009). Printed S-band 4x4 Nolen matrix for multiple beam antenna applications. *IEEE Transactions on Antennas and Propagation*, *57*(6), 1673–1678.

Garcia, R., Betancourt, D., Ibanez, A., & del Rio, C. (2005). Coherently radiating periodic structures (CORPS): a step towards high resolution imaging systems? In *IEEE Antennas and Propagation Society International Symposium*, 4B, 347–350.

Goldberg, D. E. (1989). *Genetic Algorithms in Search, Optimization, and Machine Learning*. First Ed. Reading, MA, Addison-Wesley.

Gomez, A. & del Rio, C. (2006). Obtaining images from CORPS systems. In *First European Conference on Antennas and Propagation (EuCAP)*, 1–5.

Gordon, W. (1985). A hundred years of radio propagation. *IEEE Transactions on Antennas and Propagation*, *33*(2), 126–130.

Grau, A., Romeu, J., Blanch, S., Jofre, L., & De Flaviis, F. (2006). Optimization of linear multielement antennas for selection combining by means of a Butler matrix in different MIMO environments. *IEEE Transactions on Antennas and Propagation*, *54*(11), 3251–3264.

Holland, J. H. (1992). Genetic algorithms. *Scientific American*, *267*(1), 66–72.

Hoorfar, A. (2007). Evolutionary programming in electromagnetic optimization: A review. *IEEE Transactions on Antennas and Propagation*, *55*(3), 523–537.

Hua, Y. & Sarkar, T. (1990). Matrix pencil method for estimating parameters of exponentially damped/undamped sinusoids in noise. *IEEE Transactions on Acoustics, Speech and Signal Processing*, *38*(5), 814–824.

James, R. (1989). A history of radar. *IEE Review*, *35*(9), 343–349.

Jeong, Y. S. & Kim, T. W. (2010). Design and analysis of swapped port coupler and its application in a miniaturized Butler matrix. *IEEE Transactions on Microwave Theory and Techniques*, *58*(4), 764–770.

Jin, N. & Rahmat-Samii, Y. (2007). Advances in particle swarm optimization for antenna designs: Real-number, binary, single-objective and multiobjective implementations. *IEEE Transactions on Antennas and Propagation*, *55*(3), 556–567.

Kaifas, T. & Sahalos, J. (2006). On the design of a single-layer wideband Butler matrix for switched-beam UMTS system applications [Wireless Corner]. *IEEE Antennas and Propagation Magazine*, *48*(6), 193–204.

Karimkashi, S. & Kishk, A. (2010). Invasive weed optimization and its features in electromagnetics. *IEEE Transactions on Antennas and Propagation*, *58*(4), 1269–1278.

Kennedy, J. & Eberhart, R. (1995). Particle swarm optimization. In *Proceedings of the IEEE International Conference on Neural Networks*, 4, 1942–1948.

Kennedy, J. F., Eberhart, R. C., & Shi, Y. (2001). *Swarm intelligence*. First Ed. San Francisco, CA, Morgan Kaufmann Publishers.

Khodier, M. & Christodoulou, C. (2005). Linear array geometry synthesis with minimum sidelobe level and null control using particle swarm optimization. *IEEE Transactions on Antennas and Propagation*, *53*(8), 2674–2679.

Kraus, J. (1985). Antennas since Hertz and Marconi. *IEEE Transactions on Antennas and Propagation*, *33*(2), 131–137.

Litva, J. & Lo, T. K.-Y. (1996). *Digital Beamforming in Wireless Communications*. Boston, MA, Artech House.

Liu, Y., Nie, Z., & Liu, Q. H. (2008). Reducing the number of elements in a linear antenna array by the matrix pencil method. *IEEE Transactions on Antennas and Propagation*, *56*(9), 2955–2962.

Mailloux, R. J. (1994). *Phased array antenna handbook*. First Ed. Norwood, MA, Artech House.

Marcano, D. & Duran, F. (2000). Synthesis of antenna arrays using genetic algorithms. *IEEE Antennas and Propagation Magazine*, *42*(3), 12–20.

Nedil, M., Denidni, T., & Talbi, L. (2006). Novel butler matrix using CPW multilayer technology. *IEEE Transactions on Microwave Theory and Techniques*, *54*(1), 499–507.

Panduro, M. A. (2007). Design of coherently radiating structures in a linear array geometry using genetic algorithms. *International Journal of Electronics and Communications (AEU)*, *61*(8), 515–520.

Panduro, M. A. & del Rio Bocio, C. (2008). Design of beam-forming networks for scannable multi-beam antenna arrays using CORPS. *Progress In Electromagnetics Research*, *84*, 173–188.

Panduro, M. A. & del Rio-Bocio, C. (2009). Design of beam-forming networks using CORPS and evolutionary optimization. *International Journal of Electronics and Communications (AEU)*, *63*(5), 353–365.

Panduro, M. A. & del Rio-Bocio, C. (2011). Simplifying the feeding network for multi-beam circular antenna arrays by using CORPS. *Progress In Electromagnetics Research*, *21*, 119–128.

Rahmat-Samii, Y., Kovitz, J., & Rajagopalan, H. (2012). Nature-inspired optimization techniques in communication antenna designs. *Proceedings of the IEEE*, *100*(7), 2132–2144.

Ramsay, J. (1981). Highlights of antenna history. *IEEE Antennas and Propagation Society Newsletter*, *23*(6), 7–20.

Reyna, A. & Panduro, M. A. (2008). Optimization of a scannable pattern for uniform planar antenna arrays to minimize the side lobe level. *Journal of Electromagnetic Waves and Applications*, *22*(16), 2241–2250.

Robinson, J. & Rahmat-Samii, Y. (2004). Particle swarm optimization in electromagnetics. *IEEE Transactions on Antennas and Propagation*, *52*(2), 397–407.

Rocca, P., Oliveri, G., & Massa, A. (2011). Differential evolution as applied to electromagnetics. *IEEE Antennas and Propagation Magazine*, *53*(1), 38–49.

Rose, M., Shah, S., Kadir, M., Misman, D., Aziz, M., & Suaidi, M. (2007). The mitered and circular bend method of Butler matrix design for WLAN application. In *Asia-Pacific Conference on Applied Electromagnetics (APACE)*, 1–6.

Rotman, W. & Turner, R. (1963). Wide-angle microwave lens for line source applications. *IEEE Transactions on Antennas and Propagation*, *11*(6), 623–632.

Sarkar, T. K., Wicks, M. C., Salazar-Palma, M., & Bonneau, R. J. (2003). *Smart Antennas*. First Ed. Hoboken, NJ, Wiley-Interscience : IEEE Press.

Soltankarimi, F., Nourinia, J., & Ghobadi, C. (2004). Side lobe level optimization in phased array antennas using genetic algorithm. In *IEEE Eighth International Symposium on Spread Spectrum Techniques and Applications*, 389–394.

Song, Y. & Kwon, H. (1999). Analysis of a simple smart antenna for cdma wireless communications. In *IEEE 49th Vehicular Technology Conference*, 1, 254 –258 vol.1.

Stutzman, W. & Coffey, E. (1975). Radiation pattern synthesis of planar antennas using the iterative sampling method. *IEEE Transactions on Antennas and Propagation*, *23*(6), 764–769.

Stutzman, W. L. & Thiele, G. A. (1998). *Antenna theory and design*. Second Ed. New York, NY, John Wiley & Sons.

Weile, D. & Michielssen, E. (1997). Genetic algorithm optimization applied to electromagnetics: a review. *IEEE Transactions on Antennas and Propagation*, *45*(3), 343–353.